The Role of a Member of the Transforming Growth Factor-β Family, *cet-1*, and New Signal Mediators, CeBRAM-1A and CeBRAM-2B, in the Nematode *Caenorhabditis elegans*

KIYOKAZU MORITA

DOCTOR OF SCIENCE

Department of Molecular Biomechanics
School of Life Science
The Graduate University for Advanced Studies

1999

Abbreviations

ACeDB	: a Caenorhabditis elegans data base
ActRIIA	: activin type II receptors IIA
ActRIIB	: activin type II receptors IIB
ALK	: activin receptor-like kinase
BMP	: bone morphogenetic protein
BMPRIA	: BMP receptor type I A
BRAM	: BMP receptor assosiated molecule
cat-2	: catecholamine abnormality-2
cet-1	: C. elegans TGF-β-1
C. elegans	: Caenorhabditis elegans
daf	: dauer larva formation abnormal
daf-c	: constitutive dauer formation
daf-d	: defective dauer formation
dsRNAi	: double strand RNA interference
DNA	: deoxyribonucleic acid
dpp	: decapentaplegic
dpy	: dumpy
egl	: egg laying defective
GST	: glutathione S-transferase
GFP	: green fluorescent protein
HA	: hemagglutinin
him	: high incidence of males
lon	: long
mab	: male tail abnormal
mRNA	: messenger RNA
mut	: mutator
PCR	: polymerase chain reaction
RNA	: ribonucleic acid
sma	: small
TGF-β	: transforming growth factor-β
unc	: uncoordinated

I Introduction

TGF-β superfamily and its signaling pathway

Members of the transforming growth factor -β (TGF-β) superfamily act as multifunctional ligands to control proliferation and differentiation of a variety of cell types (Kingsley, 1994). Over the past decade, many have been shown to play essential roles during early embryogenesis in a broad range of animal species (Zhou et al., 1993). More recently the ligands of TGF-β superfamily have been shown to play an important role, not only in embryogenesis, but also in morphogenesis (Meno et al., 1996; 1998) and organogenesis (Jernvall et al., 1998; Obara et al., 1999). A subfamily of these ligands, known as bone morphogenetic protein (BMP) (reviewed by Hogan, 1996), has been shown to be not only structurally but also functionally conserved across distant species. For example, human BMP is capable of rescuing a mutation in its *Drosophila* counterpart, *decapantapledgic (dpp)* (Padgett et al., 1987). Conversely, Dpp can induce ectopic bone formation in rat (Sampath et al., 1993). This extremely high conservation in the structure and function of these ligands allowed investigators to study the mechanism of their actions using multiple model animal systems such as zebrafish and ascidian (Nikaido et al., 1997; Miya et al., 1996; Miya et al., 1997). In addition to the conservation of the BMP ligands, the BMP receptor and following intracellular signaling system is also highly conserved across species (Figure 1-1A). Proper signaling requires complex formation of two distinct serine/threonine (ser/thr) kinase receptors, type I and type II. Upon ligand binding, the heteromeric complex of type I and type II receptor is formed. Type II receptor phosphorylates type I receptor at a specific sequence in the juxtatransmembrane region of the type I receptor, the (GS) box, resulting in signaling (Wrana et al., 1994; Figure 1-1A). In *Drosophila*, a homologue of vertebrate BMP-4, *dpp*, is thought to be essential not only for dorsoventral specification of the embryo (Ferguson and Anderson, 1992) but also in the patterning of imaginal discs (Nellen et al., 1996). Its action is also mediated through receptor ser/thr kinases. Three genes have so far been identified as *dpp* receptors; *tkv* and *sax* encode type I receptors (Nellen et al., 1994) and *punt* encodes a type II receptor (Ruberte et al., 1995). Genetic studies on *dpp* signaling in *Drosophila* have led to the discovery of a class of signaling molecules downstream of the *dpp* receptors. Identification of *Drosophila mothers against*

dpp (mad) (Raftery et al., 1995; Wiersdorff et al., 1996) as a downstream component of the *dpp* pathway has resulted in the isolation of a new family of vertebrate and invertebrate *Smad* genes. These *Smad* gene products play an important role in the intracellular signaling mechanisms of the TGF-β family ligands (Massague, 1996). The SMAD family consists of two classes (reviewed by Heldin et al., 1997; Figure 1-1A); pathway restricted SMADs, which include Smad1, Smad2, Smad3, and Smad5 and the common Smad4. Since Smads1 and 5, and Smads 2 and 3 act within the cells receiving the BMP, and activin or TGF-β signals, respectively in a signal dependent manner (Graff et al., 1996 ; Eppert et al., 1996), they are thought to be essential for the determination of signaling specificity. Phosphorylation of pathway-restricted SMADs by a respective type I receptor kinase has been demonstrated to be critical for their ability to mediate the signal (Zhang et al., 1996; Kretzchmar et al., 1997). A nuclear role for these transducers has been established by the demonstration that the phosphorylated SMADs translocate to the nucleus as a heteromeric complex consisting of pathway-restricted and common SMADs, and interact with transcription factors and promoter regions of target genes to regulate their expression (Chen et al., 1996; Kim et al., 1997; Lagna et al., 1996; Derynck et al., 1998; Figure 1-1A). In vertebrates, FAST-1, a winged-helix forkhead transcription factor, has been observed to associate with Smad4 in signaling-responsive transcriptional regulatory complexes (Chen et al., 1996, 1997). In human, mutations in the SMADs have been implicated in tumor progression, presumably through a lack of response to growth influencing cellular communication signals (Epport et al., 1996; Hahn et al., 1996). More recently the identification of the antagonistic SMADs, human Smad6 and Smad7 (Hayashi et al., 1997; Imamura et al., 1997; Nakao et al., 1997), and Drosophila DAD (Tsuneizumi et al., 1997) as competitive negative regulators of TGF-β-like signaling pathways has yielded an additional mechanism by which the activity of the pathway is intracellularly regulated.

***Caenorhabditis elegans* as a model animal**

Caenorhabditis elegans (C. elegans), is a small, free-living soil nematode about 1 mm in length (Figure 1-2A). They feed primarily on bacteria and have a life cycle of about 3 days under optimal condition (Figure 1-2B). They have two sexes, hermaphrodites and males. Hermaphrodites produce both oocytes and

sperm and can reproduce by self-fertilization. Males, which arise spontaneously at low frequency, can fertilize hermaphrodites.

C. elegans is a simple organism, both anatomically and genetically. The adult hermaphrodite has only 959 somatic nuclei, and adult male has only 1031. A hermaphrodite that has not mated lays about 300 eggs during its reproductive life span.

The key attributes of *C. elegans* as an excellent experimental model system for biological studies are its simplicity, transparency, ease of cultivation in the laboratory, short life cycle, suitability for genetic analysis and small genome size. The complete anatomy at electron microscope resolution and, the location and characteristics of all somatic cells in the adult hermaphrodite and male are known. More importantly, the complete cell lineage that is, the timing, location, and ancestral relationships of all cell divisions during development are known (Sulston et al., 1983). Also the structure and connection of nervous system has been completely understood by the reconstruction of electron micrographs of serial sections (White et al., 1986). A detailed knowledge of the structure of a nervous system provides insights both into the functional aspects of the structure and into the developmental mechanisms that may be used in its generation.

Genomic description of the animal, including detailed genetic mapping, cloning and analysis of mutationally defined genes, and physical mapping of entire genome is another aspect of favorable experimental attributes. Genes of *C. elegans* can be mapped into six linkage groups corresponding to the six haploid chromosomes. The haploid set includes five autosomes (A) and a sex chromosome (X). *C. elegans* genome has 97-megabase pairs. More recently, the complete genome sequence of the *C. elegans* has been revealed (The *C. elegans* Sequencing Consortium, 1998). The 97-megabase total sequence contains 19,099 predicted protein-coding genes. Approximately 42% of predicted protein products have distant matches with outside the nematode. 36% of predicted protein products of *C. elegans* have matches with human proteins. So it is worthwhile that the analysis of human homologue genes in *C. elegans*. Thus, the nematode *C. elegans* is an excellent model animal.

C. elegans TGF-β family members

In the nematode *Caenorhabditis elegans*, at least two TGF-β-like signaling

pathways exist: the dauer larva formation *(daf)* and small *(sma)* pathways (see Figure 2-5). The *daf* pathway regulates dauer larva formation in response to exposure of larval animals to starved or overcrowding conditions (Albert et al., 1981; Golden and Riddle, 1984; Figure 1-2B). Dauer larvae are stiff, motionless, and appear to be developmentally arrested. Dauer formation-defective *(daf-d)* mutants fail to form dauer larvae under starved or overcrowding conditions. In contrast, constitutive dauer formation mutants *(daf-c)* are unable to resume a normal life cycle after the dauer-stimulating conditions are removed (Figure 1-2C). Seven genes, *daf-1, daf-3, daf-4, daf-5, daf-7, daf-8,* and *daf-14* have been proposed to act in a common signaling pathway in the regulation of dauer larva formation (Thomas et al., 1993; Figure 1-2C). *daf-c* genes, *daf-1* (Georgi et al., 1990) and *daf-4* (Estevez et al., 1993) encode type I and type II ser/thr kinase receptors for the TGF-β superfamily, respectively. DAF-4 has been shown to bind to BMP-2 and BMP-4 in mammalian cells (Estevez et al., 1993). More recently, DAF-7, also a member of the TGF-β superfamily, has been reported to negatively regulate dauer larva formation. Loss of function *daf-7* mutants display a Daf-c phenotype (Ren et al., 1996). Molecular analysis of *daf-d* genes, *daf-3,* which can suppress the phenotypes of *daf-1, daf-4, daf-7, daf-8, and daf-14,* has been shown to encode an inhibitory SMAD protein (Patterson et al., 1997). On the other hand, the *sma* pathway appears to control nematode body length as well as ray formation in the male tail. Mutants of *sma* such as *sma-2, sma-3,* and *sma-4* have shortened body length (Sma), and male tail abnormal (Mab) phenotypes (Baird and Emmons, 1990). *sma-2, sma-3,* and *sma-4* have been shown to encode proteins similar to the SMADs identified in *Drosophila* and vertebrates (Savage et al., 1996). Interestingly, *daf-4,* which acts in the *daf* pathway also seems to be involved in the *sma* pathway. *daf-4* mutants display both Sma and Mab phenotypes. Mosaic analysis demonstrated that *sma-2* functions cell-autonomously and is downstream of *daf-4* (Savage et al., 1996).

The male tail of *C. elegans* provides another model for studying TGF-β signaling. The male tail is a fan-shaped structure required for copulation, consisting of nine bilateral pairs of peripheral organs (sensory rays) formed in a precise pattern from the adult lateral epidermis (Sulston et al., 1980). The specification of ray identity has been shown to be a very complex process involving many genes. *mab-5* and *egl-5,* which encode homologues of *Drosophila*

antennapedia and *abdominal-B*, respectively, were reported to be involved in cell fate determination of the sensory rays (Chow et al., 1994; Cowing and Kenyon, 1996). Changes in the expression of MAB-5 protein, in particular its on-off switching, in the same cell lineage, is critical for proper region-specific patterning (Salser and Kenyon, 1996). The *mab-21* gene, which encodes a novel protein, has been shown to be involved in the regulation of ray 6 identity (Chow et al., 1995). *mab-21* mutants exhibit transformation of ray 6 to ray 4 identity which results in subsequent ray fusion. In contrast, *sma-2*, *sma-3*, *sma-4*, and *daf-4* mutants usually have ray 4-9 showing a fat morphology. Rays 4 and 5, ray 6 and 7 as well as ray 8 and 9 often fused to form fat rays (Baird et al., 1991; Savage et al., 1996). This implies that MAB-21 may be a component that can interact antagonistically with the *sma* pathway in determination of the ray morphology.

In this study, I first report the identification of the novel TGF-β like ligand *cet-1*, in *C. elegans* and its function by isolation of the *cet-1* null mutant in Part 1 (Morita et al., 1999). *cet-1* is the ligand of the *sma* pathway in *C. elegans* and regulates the body length as a dose dependent manner. In Part 2, I demonstrate the identification of the two genes, CeBRAM-1A and CeBRAM-2B, the homologues of human type I receptor binding protein BRAM-1 (BMP receptor associated molecule-1) in *C. elegans*. I also isolated and characterized these null mutants. Finally, I propose the role of new signal mediators, CeBRAM-1A and CeBRAM-2B, of two conserved TGF-β signal pathways in *C. elegans*.

Part I

Regulation of Body Length and Male Tail Ray Pattern Formation of *Caenorhabditis elegans* by a Member of TGF-β Family, *cet-1*

II-1 Summary

I have identified a new member of the TGF-β superfamily, CET-1, from *Caenorhabditis elegans*. *cet-1::GFP* is expressed in the ventral nerve cord and other neurons. I isolated *cet-1* null mutant by Tc1 deletion method. *cet-1* null mutants have shortened bodies and male tail abnormal phenotype resembling *sma* mutants. These results suggest that *cet-1*, *sma-2*, *sma-3*, and *sma-4* share a common pathway. Overexpression experiments demonstrated that *cet-1* function requires wild type *sma* genes. Interestingly, CET-1 appears to affect body length in a dose dependent manner. Heterozygotes for *cet-1* displayed body lengths ranging between null mutant and wild type, and overexpression of CET-1 in wild type worms elongated body length close to *lon* mutants. Furthermore, my results show that *cet-1* controls body length not proportionally but in two particular regions of the worm probably by changing cell volume. Moreover, genetic interaction of the *cet-1* with mutants of the other TGF-β pathway in *C. elegans*, *daf* demonstrated that *cet-1* is also involved at least partly in the *daf* signaling pathway. In male sensory ray patterning, lack of *cet-1* function results in ray fusions. Epistasis analysis revealed that *mab-21* lies downstream and is negatively regulated by the *cet-1/sma* pathway in the male tail. My results show that *cet-1* controls diversed biological processes during *C. elegans* development probably through different target genes.

II-2 Introduction

In *C. elegans*, mutations that result in small body size and abnormal male tail structure (Mab phenotype) have identified components of a putative TGF-β signal transduction pathway termed the Sma/Mab pathway (reviewed in Padgett et al., 1998). The *daf-4* and *sma-6* genes encode type II and type I receptors, respectively (Estevez et al., 1993; Krishna et al., 1999). The *sma-2*, *sma-3*, *sma-4* genes encode Smad proteins (Savage et al., 1996).

DAF-7 inhibits entry into and promotes recovery from the dauer state, an alternative third larval (L3) diapause stage adopted by animals developing under conditions of starvation or overcrowding, or both (Ren et al., 1996). A second TGF-β family member, UNC-129, directs axon guidance (Colavita et al., 1998).

In this study, I identified a gene encoding a new TGF-β family member, *cet-1*. By means of deletion mutations and genetic analysis, I demonstrate that *cet-1* is a ligand for the *sma* pathway and can regulate the *C. elegans* body length in a dose dependent manner. I also show by epistatic analysis that the regulatory cascade of the *sma* pathway is highly conserved and negatively acts on *mab-21* during male tail patterning. I provide evidence that *cet-1* may also be involved in the *daf* pathway and will discuss the possibility of cross-talk between the *daf* and *sma* pathways at the level of ligand binding.

II-2 Results

Isolation and characterization of *cet-1* cDNA

The structure and function of the TGF-β family ligands are known to be highly conserved among animal species, so I designed degenerate oligonucleotide primers corresponding to conserved sequences within the C-terminal region of the vertebrate BMPs (Basler et al., 1993). Using these primers, I was able to amplify a 116 bp PCR fragment encoding a BMP-related sequence from cDNA derived from mixed stages of *C. elegans*. This fragment was used as a probe to screen a mixed stages cDNA library from which one positive clone was obtained from 6 X 10^6 plaques. Sequence analysis revealed that the clone contains a typical SL1 sequence (Huang and Hirsh, 1989) at the 5' end. Because Northern blot analysis indicated a transcript of about 1.8 kb in length, the isolated clone of approximately 1800 bp most likely represents a full length transcript. This clone contains a single open reading frame of 1768 nucleotides predicting a polypeptide of 365 amino acids (Figure 2-1A).

To date, two TGF-β-related ligands have been reported in *C. elegans*, DAF-7 and UNC-129 (Ren et al., 1996; Colavita et al.,1998). The predicated amino acid sequence identified this gene product as distinct from DAF-7 or UNC-129 and thus, it represents a novel member of the TGF-β superfamily in the nematode. We named this new gene as *cet-1* (*C. elegans* TGF-β-1). It contains a RRKR sequence (underlined, position 233-236), a potential cleavage site for furin-like enzymes (Dubois et al., 1995) for the release of C-terminus of the polypeptide. In addition, the predicted mature protein of 129 amino acids in the C-terminus contains a conserved distribution of cysteine residues that is characteristic to TGF-

β family members. Comparison of the amino acid sequence of CET-1 with other members of this family revealed that CET-1 is more closely related to members of the Vg1, DPP and BMP subfamily than to the TGF-β and activin subfamilies, and closest to Nodal in the region of the predicted mature peptide (Figure 2-1 B). When the phylogenetic tree was depicted by computer-assisted analysis based on the amino acid sequence of the C-terminal region (which are conserved within TGF-β superfamily), CET-1 was placed closest to Nodal, although it also shares high similarity with BMP-2/4 (Figure 2-1C).

I examined the ability of CET-1 to function in the *Xenopus* embryo, taking advantage of the conserved function of TGF-β related factors across species. Overexpression of *cet-1* mRNA in the ventral blastomeres of *Xenopus laevis* caused duplication of the dorsal axis. This result classifies CET-1 with activin, Vg1, Nodal and Nodal-related (NR) for the ability to induce a secondary body axis, when overexpressed ventrally (Thomsen et al., 1990). It differs from the other group of TGF-β like molecules including the BMP-2/4, which ventralize embryos upon overexpression dorsally (Dale et al., 1992). This axis inducing ability of CET-1, together with the structural information, indicates that CET-1 belongs to the Nodal subfamily rather than BMP-Dpp family gene. Alternatively, overexpressed CET-1 which may not be processed properly in vertebrate, might cause a dominant negative effect on endogenous BMPs. Thus, the possibility that CET-1 belongs to BMP-2/4 subfamily cannot be completely ruled out.

I next determined the genetic and physical map positions of the *cet-1* gene. Analysis of the genomic structure showed that the *cet-1* gene consists of eight exons. Search of the *C. elegans* database revealed that the genomic sequence of *cet-1* is contained within cosmid T25F10, which has been mapped on linkage group V (Figure 2-1D). However, no known mutants have yet been localized in this region.

***cet-1::GFP* fusion reveals its expression pattern in wild type animals**

To examine the expression pattern of *cet-1 in vivo* at the cellular level, I generated transgenic worms expressing a *cet-1::GFP* fusion gene. Transgenic worms expressing this fusion protein under regulation of the *cet-1* promoter displayed green fluorescence in many neurons, including some amphid neurons and neurons in ventral nerve cord (VNC) (Figure 2-2A). The cell bodies of VA,

VB, DA and DB neurons were detected with fluorescence (Figure 2-2B). The amphid neuron identified was AFD. Body wall muscles and neurons in the pharyngeal region was also detected (Figure 2-2C). Signal was detected in cell bodies of another neuron, the canal associated neuron (CAN) (Figure 2-2D), and DVA neuron at the anal region of the tail (Figure 2-2E). Male-specific expression was observed in the neurons of the tail region (Figure 2-2F). This expression pattern persisted through L1 to adult hermaphrodite. Interestingly, CET-1 is broadly expressed in neurons in contrast to DAF-7, that is thought to act like as a neurotransmitter and whose expression is restricted to amphid neuron ASI (Ren et al., 1996; Schackwitz et al., 1996).

***cet-1* null mutant shows small phenotype.**

To investigate the functional role of *cet-1*, I utilized the strategy of gene disruption by insertion of a Tc1 transposable element in the *cet-1* region. Subsequent excision and transposition of Tc1 would likely result in a deletion of the functional domains of the targeted gene (Zwaal et al., 1993). I screened pools of potential mutants for sucessful insertion of the Tc1 transposon in the region of *cet-1* gene by polymerase chain reaction (PCR) using specific oligonucleotide primers. Figure 2-3A shows one case in which Tc1 was inserted into the 5' region 4081 bp upstreamof the first methionine of the *cet-1* coding region. I then screened for worms in which transposition of Tc1 caused deletions that might affect the function of CET-1. I isolated two deletion alleles, *kk3* (c) and *kk4* (b). *kk3* which had a deletion of a 5690 bp including almost all the exons of *cet-1*, showed a Sma phenotype (Figure 2-3B; Table 2-1), while *kk4*, in which 1846 bp was deleted in the 5' untranslated region, exhibited no obvious abnormalities nor change in body length (Table 2-1). The average body length of an adult *cet-1(kk3)* mutant was 0.75 mm, which is comparable to that of known *sma* pathway mutants such as *sma-2*, *sma-3*, *sma-4*, and *daf-4*. Because of the deletion of the entire *cet-1* coding region in this allele, we believe that *kk3* represents a null allele of the *cet-1* gene.

CET-1 regulates *C. elegans* body length in a dose dependent manner.

To get further insight into the regulation of the *C. elegans* body length, I compared the lengths of 5-day old hatched hermaphrodites of N2 wild type and various mutants. In the cases of wild type and *daf-7* mutant, the body lengths

ranged from 1.27 to 1.28 mm, respectively (Table 2-1). In the small phenotype mutants including *daf-4*, the body lengths of corresponding adult worms fell in the range of 0.71 to 0.81 mm. *sma-2(e502)* and *sma-3(e491)* have missense mutations in which an essential highly conserved glycine residue is substituted with other amino acids, resulting in strong loss-of-function alleles (Hoodless et al. 1996). Therefore, it is possible that the shortened body lengths of *sma-2*, *sma-3*, and *sma-4* mutants are due to the decrease in Smad signals to almost background level, similar to our *cet-1(kk3)* null mutant. *daf-7* background does not seem to affect the body length, because the body lengths of *daf-7(m 62)* mutant are nearly wild type, and those of *daf-7(m 62); cet-1(kk3)* double mutant are indistinguishable from *cet-1(kk3)* alone.

I also examined whether a plasmid construct encoding the genomic DNA that covers the region deleted in *cet-1(kk3)* could rescue the null mutant upon DNA injection. The shortened body length distinctive of the Sma phenotype, was rescued to normal length by overexpression of exogenous *cet-1* gene in a dose dependent manner (Table 2-1). When injection of a high concentration of the *cet-1* plasmid was performed, rescued animals, *cet-1(kk3); kkEx8[cet-1(+) 10:1]*, had an average rescued body length of 1.15 mm. On the other hand, when injection was performed at a lower dose, rescued animals, *cet-1(kk3); kkEx9[cet-1(+) 100:1]*, were average of 1.04 mm in length. In addition, overexpression of *cet-1* in wild type animals resulted in a *lon* (Long) phenotype (average body length of 1.43 mm) resembling the elongated body seen in *lon-1* and *lon-2* mutants. Furthermore, overexpression of *cet-1* in *lon-1* mutants resulted in even longer worms, although with quite low viability. Heterozygous *cet-1* mutant worms *(cet-1/+)*, in which the dosage of *cet-1* is half the level of wild type, are shorter in length (1.12 mm) than wild type, but longer than the *cet-1* homozygous (*cet-1/cet-1*) mutant. Taken together, these results suggest that CET-1 can control the body length of *C. elegans* in a dose dependent manner.

Regional difference in body length shortening and elongation.

To determine the qualitative changes in body length, I measured the individual lengths of each body region. Comparison of *cet-1(kk3)* mutants with N2;*EX10[cet-1(+)]* worms, shows an overall change in body length of almost two fold (0.75 to 1.43 mm) (Table 2-1). Interestingly, the length of the pharynx was not drastically affected; the relative lengths of the pharynx to total length were 9 and

13% in *cet-1(kk3)* and N2;*EX10[cet-1(+)]*, respectively (Table 2-3). The measurement is comparable to that of wild type N2 (11%) (Table 2). In contrast, the length of pharynx to gonad, and gonad to anus were remarkably expanded 5 to 10 fold between *cet-1(kk3)* and N2;*EX10[cet-1(+)]* (2 to 22% and 3 to 19 %, respectively) (Table 2-4). Figure 2-4 shows the tail region of a DAPI-stained wild type worm (A) in comparison with a *cet-1(kk3)* mutant (B) and N2;*EX10[cet-1(+)]* mutant (C). The length between the posterior edge of the gonad arms and anus is distinctively elongated. Upon the extension of this region, the space between the nuclei of hyp7 cells was expanded. Similar gross changes in overall morphology can be seen in a variety of *C. elegans* mutants, including Blister, Roll, and Dumpy. These mutants are known to be defective in cuticle function with altered collagen structure. Therefore, one explanation for the changes of body length in the *cet-1* mutant may be that the level of CET-1 protein can regulate the synthesis and deposition of extracellular scaffold components such as collagen.

cet-1 function requires wild type _sma_ genes.

Because the null mutant of *cet-1* shows an indistinguishable phenotype from those of *sma-2*, *sma-3*, and *sma-4*, we carried out an epistatic analysis by injecting the genomic fragment capable of rescuing *cet-1* into *sma-2*, *sma-3*, and *sma-4* mutants. The *cet-1* genomic fragment failed to rescue the *sma-2*, *sma-3*, and *sma-4* mutant phenotypes. These results indicate that CET-1 likely acts upstream of SMA-2, SMA-3, and SMA-4. *cet-1* function, either in wild type background or when it is overexpressed, requires the SMAD proteins to transduce the signal.

cet-1 null mutant shows male tail abnormality

In addition to the shortened body length, *cet-1(kk3)* mutants exhibited abnormalities in the male tail. Crumpled spicules were found in almost all the males (38/40). More profound phenotype was also observed in the patterning of the sensory rays (Figure 2-4C, D). The majority of tails had fusions of rays 4 and 5, rays 6 and 7 as well as rays 8 and 9 resulting in fat fused rays (Figure 2-4D). This ray fusion was often observed on both sides of the body (Table 2-3). In rare cases, multiple fusions at 4 and 5, 6 and 7, and 8 and 9 occurred laterally. These phenotypes are also reminiscent of those in *sma-2*, *sma-3*, *sma-4 and daf-4* mutants. However, the higher frequency and severity of ray fusions seen in the *cet-1(kk3)* mutant, as compared to those of known *sma* pathway mutants, suggests

that *cet-1* has more severe effect than single mutations of *Smad* genes.

mab-21 is epistatic to genes in the _sma_ pathway and is negatively regulated by _cet-1_.

In *sma* pathway mutants, ray 4, 5 and 7 which are normally thin rays become fat rays like ray 6. Fusion between these rays are observed frequently. Mutation of *mab-21* results in specific transformation of ray 6 into a more anterior ray 4. The displacement of the transformed thin ray 6 leads to the formation of a very thick ray in which both thin ray 6 and 4 are fused (Baird et al., 1991; Chow et al., 1995). This transformation appears opposite to the phenotype of mutants in the *sma* pathway. To analyze the relationship between *sma* and *mab-21*, I constructed double mutants of *sma* pathway mutant and *mab-21*. Table 2-4 shows that *mab-21* is epistatic to all of the *sma* pathway mutants for ray pattern formation, indicating that *mab-21* is downstream of the *sma* pathway and is negatively regulated by *cet-1*. In the absence of *mab-21* product, the generation of thick ray in the small mutants could not be accomplished. However, it is interesting to note that while *mab-21* mutant phenotype suppressed the Mab phenotypes of *sma* pathway genes, the body length of the double mutants remained short. These results suggest that sensory ray patterning and body length regulation are acting through the *sma* pathway, but bificate at the control of their target genes.

Because *mab-21* is necessary for determination of the identity of ray (Chow et al., 1995), I analyzed the expression pattern of *mab-21::GFP* in wild type and *cet-1* null mutant backgrounds to see if expression level or pattern is altered in the mutant. *mab-21* reporter gene is expressed in the structural and hypodermal cells of ray 2 to ray 7. In the *cet-1* null mutant background, the expression pattern was not altered as compared with that in wild type. While no significant increase of gene activity was detected with the reporter, and no additional cell expressing the reporter gene was noticed, the results suggest that the mechanism which *cet-1* signal inpinges on the *mab-21* activity may not be acting at the transcriptional level.

CET-1 interacts with the *daf-7* TGF-β pathway

As mentioned above, there are two distinct TGF-β pathways in *C. elegans*.

To examine whether the *cet-1/sma* pathway cross-talks with the *daf* pathway at the level of ligand-receptor interaction, I generated double mutants of *cet-1* and *daf-7*. Dauer formation of the *daf-c* mutant is stimulated at non-permissive temperature even under healthy growth and feeding conditions. *daf-7* mutants show Daf-c phenotype and constitutively form dauer larvae at 20 and 25° C (Table 2-5). At 20° C, 21% of both *daf-7(e1372)* and *daf-7(m62)* mutants formed dauer larvae, and this dauer formation was enhanced in the double mutants of *daf-7(e1372); cet-1(kk3)* and *daf-7(m62); cet-1(kk3)* at a frequency of 77 and 56%, respectively, suggesting that *cet-1* may also be participating as a suppressor of dauer formation in combination with *daf-7*. To examine whether this interaction occurs at the ligand-receptor level or the intracellular signaling level, downstream of the receptor, I constructed *daf-7; sma-2* double mutants. Since *sma-2* is known to act as an intracellular signaling component of the *sma* pathway, we hypothesize that if the interaction between *cet-1* and *daf-7* acts through the intracellular signals, *daf-7; sma-2* double mutants should also result in an increased penetrance of the Daf phenotype at 20° C. Table 2-5 shows that the interaction between *daf-7* and *sma-2*, if it is present, is a rather weak one. It argues that *cet-1* is interacting with the *daf* pathway extracellularly at the ligand receptor level. This, in turn suggests that CET-1 may interact with a complex of receptors comprising of DAF-1, DAF-4 or SMA-6 and participate in the regulation of *daf* pathway. However, I cannot rule out the potential presence of cross-talk occurring within the cell at the level of SMAD proteins.

II-4 Discussion

CET-1 is a ligand in the *sma* pathway.

In the past several years, genetic studies in *C. elegans* have identified at least 5 components, *sma-2, sma-3, sma-4, sma-6* and *daf-4*, involved in the *sma* pathway (Savage et al., 1996; Krishna et al., 1999). However, the ligand(s) that triggers the signaling pathway was unknown. In this study, I show that a newly identified gene, *cet-1*, encodes a ligand for the *sma* pathway. I was able to demonstrate that its null mutation resulted in Sma and Mab phenotypes reminiscent to mutants of *sma-2, sma-3, sma-4, sma-6,* and *daf-4*. The same phenotype was also observed independently in two other *cet-1* alleles (Suzuki et

al., 1999). In addition to the *sma* pathway, recent studies have identified components that mediate the *daf* pathway; DAF-7 as a ligand; DAF-1 as a type I receptor; DAF-4 as a type II receptor; and DAF-3 as SMADs. It appears that DAF-4 functions as a common type II receptor for both *sma* and *daf* pathways. By analogy with the dual role of activin type II receptors IIA (ActRIIA) and IIB (ActRIIB) being utilized in both activin and BMP pathways in vertebrates (Schulte-Merker et al., 1994; Oh et al., 1997), DAF-4 has been suggested to function similarly in mediating signals from multiple ligands. DAF-7 has 9 conserved cysteine residues in the predicted mature peptide, which place it in the TGF-β or activin subfamily (Ren et al., 1996). In contrast, CET-1 has only 7 cysteine residues, like the BMP *dpp* subfamily members. In this regard, it is interesting to note that the dual specificity of the common type II receptor in recognizing two types of ligand, is also conserved between *C. elegans* DAF-4 and vertebrate ActRIIs.

Taken together, I propose that in *C. elegans* there are at least two TGF-β-like pathways which are triggered by distinct ligands, DAF-7 and CET-1. Each of these pathways uses a pathway-specific type I receptor, a common type II receptor, DAF-4, and receptor-specific SMAD-like components (Figure 2-5). In this study, I have demonstrated a genetic interaction between *daf-7* and *cet-1*, suggesting that the CET-1 ligand is not exclusively utilized for the *sma* pathway but can also participate in the *daf* pathway, if it is minimal (arrow with broken line Figure 2-4). Such a functional redundancy of the TGF-β family ligands has previously been reported for activin and OP-1 (BMP-7), both of which are capable of inducing dorsal mesoderm in animal caps of early *Xenopus* embryo through a common type I receptor ALK2 (ActRI) and ActRIIA (Yamashita et al., 1995).

How body length is determined by CET-1.

It is intriguing to find that body length in *C. elegans* can be controlled by CET-1 in a dose-dependent manner. Namely, the extent to which the shortened body length of *cet-1* mutants could be rescued was dependent upon the amount of exogenous *cet-1* introduced. In addition, *lon* mutants as well as N2 wild type worms could be elongated by overexpression of CET-1. Absence or reduction of the CET-1 level to half of that in the wild type animal also resulted in shortening of body length proportionally. The exact molecular mechanism by which body length is determined remains to be solved. However, it is clear that a diffusible

signaling molecule can act as modifier of the developmental regulation. The total amount of CET-1 ligand present in an individual worm might guide the determination of the body length.

The use of the *cet-1::GFP* fusion construct allowed observation that CET-1 expression in hermaphrodites is mainly neuronal, in the amphid neurons and ventral nerve cord, and that this expression remains consistent throughout the four larval stages and in adults. The DAF-4 type II receptor, an essential component of the *sma* pathway, is broadly expressed in many anterior pharyngeal and tail neurons, ventral nerve cord, intestine, and pharynx as revealed by *daf-4::GFP* (Patterson et al., 1997). This observation is consistent with the idea that this receptor is used not only in the *sma* but also in the *daf* pathway. It is therefore unlikely that DAF-4 expression would determine the regional specificity of CET-1 activity. In contrast to DAF-4, *sma-6::GFP* is expressed mainly in anterior pharyngeal and tail hypodermis (Krishna et al., 1999). Given that the signaling specificity of the TGF-β pathway is determined by type I receptors (Wrana et al., 1992), regional activation of the *sma* pathway may be determined by restricted expression of the SMA-6 type I receptor. On the other hand, hypodermal cells are known to form syncytium. Therefore, signals from the receptor might also be regionally restricted by localized effectors downstream of SMA-6. I thus hypothesize that the target cells lie in the hypodermis of anterior pharyngeal and tail regions where SMA-6 is expressed.

The next question to address is why the body length is controlled by the amount of CET-1. Morphological changes, including alteration of body length, often attribute to defects in cuticle formation. For example, mutations in *dpy-2*, *dpy-7*, and *dpy-10*, all of which encode collagen (Levy et al., 1993; Johnstone et al., 1992), a major component of cuticle, result in a short body length and dumpy phenotype. These results suggest that cuticle formation might be altered depending on the dosage of CET-1 ligand. CET-1 belongs to the dpp/Vg1 subfamily, are believed to be poorly diffusible, when being examined in cultured cells. They have the tendency to be retained on the surface of expressing cells due to attachment to extracellular matrix (Panganiban et al., 1990). In *Drosophila* wing discs, however, DPP can act as a morphogen and influence the behavior of cells positioned over 20 cells away. This response is thought to be due to the direct action of the secreted DPP protein (Nellen et al., 1996), although it might also involve cell proliferation and cell communication. In my case, while the target

tissue is a hypodermal syncytium, the CET-1 can act through extracellular diffusion to reach the specific receptor. Diffusion of the intracelluar signaling components, such as the SMAD proteins, can also facilitate further propagation of developmental signal within regional domains of the hypodermal sheath. The proportional alteration of the body length in specific region in mutant animals would certainly argue for this notion.

Male tail ray pattern formation

mab-21 acts as a component that regulates pattern formation of male tail ray by directing seam cells to become specific ray during the late L3 and early L4 larval stages (Chow et al., 1995). I demonstrate that *mab-21* acts downstream of the *sma* signaling pathway, and is negatively regulated by *cet-1*. In the male tail of double mutants of *mab-21* and *sma* genes, only *mab-21* mutant ray pattern was displayed. This fat to thin ray transformation phenotype in the absence of *sma* pathway genes implies that the fat ray morphology requires functional *mab-21* gene product. My results on the *mab-21* reporter gene expression argues that the negative regulation of *mab-21* by *cet-1* may be at the posttranscriptional level. In wild type animal, *mab-21* expression is present in the V6 rays and ray 7. Among these, only ray 6 can bypass the repression by the *cet-1* signal and take up a fat morphology. In the other rays, however, *mab-21* function is suppressed by the *cet-1* signal. Thus, they all take up a thin morphology. Upon mutations of the *sma* pathway components, the repression is relieved, and upregulation of the *mab-21* biological activity leads to a thin to fat morphology transformation. On the other hand, in the absence of *mab-21* gene function, the repressing signal becomes irrelevant. All the rays become thin. The issue would lie on what makes ray 6 different from the rest. Although it remains speculative, *mab-5*, *egl-5* and *mab-18* (Chow and Emmons, 1994), which encode *antennapedia*, *abdominal B* type homeobox containing proteins (Wang et al., 1993) and a *Pax-6* homologue (Zhang and Emmons, 1995), respectively, would be strong candidates that help defining the uniqueness of ray 6 in response to the repressing signal.

mab-21 gene is highly conserved in various animal species from vertebrates to invertebrates (Margolis et al., 1996). In vertebrates, its expression is most prominent in the brain, and in *C. elegans*, *mab-21* is expressed mainly in neuron, hypodermis and ray cells. These observations suggest that *mab-21*, which is acting downstream of TGF-β type signal, may be involved in the regulation of

neuronal/hypodermal development. In addition, *mab-21* is thought to be the functional modulator of the homeobox genes *mab-5*, *egl-5* and *mab-18* . Since Hom-C/Hox genes are the key players in cell fate decision and body patterning, my results suggest that male tail may provide a good model system to examine how upstream regulatory signals like the *cet-1* ligand can pattern the sensory rays through these homeodomain containing transcription factors and their modulators.

Bifurcation and convergence of signals.

From the epistatic analysis, *mab-21* mutant phenotype suppresses the ray patterning defects of the *sma* pathway mutants. However, suppression does not occur with regard to the body length abnormality. My results argue that body morphology regulation and the ray patterning are two distinct processes in normal nematode development. The specificity of these biological responses is not modulated by the signaling molecules. These processes act through a common extracellular ligand secreted from neurons, common receptors and intracellular SMAD molecules in the target cells. It is through different target genes present in these cells at a specific time frame that alternative but specific responses are generated.

Variation on expressivity of phenotype of mutant signaling molecule can be found in the *daf* pathway. Null mutant *daf-7* strain exhibits a temperature sensitive Daf-c phenotype. It suggests more than only the temperature sensitivity of wild-type dauer formation process (Golden and Riddle 1984) but also the potential presence of an alternative dauer inductive signal. Although *cet-1* mutation alone gives no indication of its role in dauer formation, my double mutant analyses clearly illustrate that *cet-1* can be that second signal (see table 2-5). In fact, similar phenomenon is also found in ray patterning. While the degree of ray fusions in *cet-1* null mutants are significantly higher than those of *sma-2*, *sma-3*, *sma-4* and *daf-4* mutants, the severity still varies among individuals. It implies that an alternative ray patterning signal may be present. The recent identification of a novel TGF-β like ligand UNC-129 (Colavita et al.,1998) eludes to the presence of a related molecule that may act in concert with *cet-1* in certain developmental processes, although their cooperative functionality remains to be tested.

III Part 2

CeBRAM-1A and CeBRAM-2B, New Signal Mediators of TGF-β Signaling Pathways in the Nematode *Caenorhabditis elegans*

III-1 Summary

I have identified two genes, CeBRAM-1A and CeBRAM-2B, which are similar to human BRAM-1 previously identified as a BMP receptor associated molecule, in *C. elegans*. The *C. elegans* BRAMs (CeBRAM-1A and CeBRAM-2B) show significant amino acid identity with human BRAM-1, particularly in the C-terminal region. CeBRAM-1A was found to associate with DAF-1, the type I receptor in the *daf* pathway in *C. elegans* as well as a vertebrate BMP type I receptor BMPRIA. *CeBRAM-1A::GFP* fusion protein is expressed mainly in amphid neurons such as ASK, ASI, and ASG etc, where DAF-1 is expressed. Loss-of-function of CeBRAM-1A gene showed that the mutant worms looked normal except that they showed a behavior of head-lifting phenotype. Genetic interaction of CeBRAM-1A with previously known *daf-7* TGF-β pathway mutants revealed that CeBRAM-1A negatively regulates the *daf-7* TGF-β pathway and functions between *daf-1* type I receptor and *daf-14* SMAD. On the other hand, *CeBRAM-2B::GFP* fusion protein was expressed strongly in pharyngeal muscle and intestinal cells. This expression pattern of CeBRAM-2B is similar to that of *sma-6* type I receptor of the *cet-1/sma* pathway. Interestingly, double strand RNA interference (dsRNAi) of CeBRAM-2B showed Lon phenotype. These results strongly suggest that CeBRAM-1A and CeBRAM-2B may function as negative regulators of two distinct TGF-β signal pathways, the *daf* pathway and the *sma* pathway respectively in *C. elegans*. Thus, I propose that CeBRAM-1A and CeBRAM-2B define a novel class of molecules that serve as a negative regulator of TGF-β pathways acting downstream of the type I receptor.

III-2 Introduction

Many of genes that control cell growth and differentiation in mammalian have been shown to have structural and functional homologues in simpler model organisms such as *Droshophila* and *C. elegans*. The nematode *C. elegans* is the most thoroughly understood multicellular animal in terms of cellular development, anatomy, and genome structure. This allows us to use genetic approaches for the understanding of conserved signaling pathway of cell-to-cell interactions that regulate developmental processes.

Recent studies on action mechanism of TGF-β superfamily identified several molecules essential for the signaling (reviewed by Heldin et al., 1997). They include type I and type II serine/threonine (ser/thr) kinase receptors, SMADs, and transcriptional regulators that cooperate with SMADs. Particularly studies on bone morphogenetic proteins (BMPs) (reviewed by Hogan 1996) whose functions are essential in early embryogenesis and highly conserved among species, contributed significantly to the elucidation of intracellular signaling of the whole family .

Recently, molecules associated with several TGF-β family receptors have been identified. One such a molecule, the immunophilin FKBP12, has been reported to interact with TGF-β family type I receptors (Wang et al., 1994; Wang et al., 1996; Huse et al., 1999). FKBP12 binding to type I receptors may function to suppress spurious signaling by inhibiting spontaneous interaction between TGF-β receptor type I and TGF-β receptor type II. Crystal structure of the cytoplasmic domain of the TGF-β receptor type I in complex with FKBP12 reveals that FKBP12 binds to the GS domain of type I receptor and protects the TGF-β receptor type II phosphorylation sites and stabilize the inhibited conformation of the kinase (Huse et al., 1999). The α subunit of farnesyl-protein transferase (FT-α) was also isolated as a TGF-β receptor type I associated molecule (Kawabata et al., 1995). Farnesyltransferase is known to play a critical role in the activation of p21RAS by attaching to it a farnesyl group, which facilitates its membrane association. Although FT-α has been shown to be phosphorylated by TGF-β receptor type I, the functional role of this modification is not clear.

More recently, a group of proteins, the Smad, have been identified as important components of the TGF-β superfamily signal transduction pathway in a variety of species (Graff et al., 1996). In vertebrate, Smad1 and Smad5 have been shown to mimic the effect of BMP-2/4 in *Xenopus* as well as in mammalian cells. Smad2 and its close isoform Smad3 mediate signaling elicited by TGF-β or activin. In human, Smad4/DPC4, originally isolated as a tumor-suppressor gene on chromosome 18q21(Hahn et al., 1996), function in cooperation with Smad1, Smad2, and Smad3 as a common mediator of signaling elicited by members of the TGF-β superfamily. Although Smads have been shown to be critical for TGF-β

superfamily signaling, it is not clear whether other factors are also involved in their nuclear translocation and following transcriptional regulation.

To understand molecular mechanism of BMP signaling in more detail, we attempted to identify components that may modulate BMP signaling triggered by BMP receptors. Using the yeast two-hybrid screening system, we have recently isolated a human gene encoding a protein that binds to BMP receptor type I (BMPRIA/ALK3) (ten Dijke et al., 1994 ; Suzuki et al., 1994), and designated it as BMP receptor associated molecule-1 (BRAM-1) (Kurozumi et al., 1998). hBRAM-1 was found to be an alternatively-spliced form of BS69, a previously identified adenovirus E1A-associated protein (Hateboer et al., 1995). Hateboer et al. reported that BS69 binds to the transactivation domain of E1A and specifically inhibits its transactivation function. However, we demonstrated that BS69 does not bind to any type I receptors of TGF-β family. Although the cytoplasmic protein human BRAM-1 has been shown to bind specifically to BMPRI-A, *in vivo* function was not clear.

In the *C. elegans*, at least two TGF-β like signaling pathways exist (see Part 1; Figure 2-5): the dauer larva formation (*daf*) and small (*sma*) pathways. The former pathway regulates formation of dauer larva in response to exposure of larval animals to starve or overcrowding conditions (Albert et al., 1981; Golden et al., 1983; Figure 1-2B). Dauer constitutive (*daf-c or daf-d*) genes such as *daf-1, daf-3, daf-4, daf-5, daf-7, daf-8,* and *daf-14* have been proposed to act in a common pathway in the regulation of dauer larva formation (Georgi et al., 1990 ; Estevez et al., 1993 ; Ren et al., 1996 ; Patterson et al., 1997 ; Thomas et al., 1993; Figure 1-2C). The latter pathway appears to control nematode body length as well as ray pattern formation in the male tail (Servage et al., 1996 ; Krishna et al., 1999; Morita et al., 1999; Suzuki et al., 1999). Therefore, it was expected that CeBRAM-1A and CeBRAM-2B that are similar to vertebrate BRAM-1 are involved in the regulation of either pathway.

In this study, I identified two genes, CeBRAM-1A and CeBRAM-2B which are similar to human BRAM-1, in *C. elegans* by searching a data base. *CeBRAM-1A::GFP* was expressed in mainly neurons. CeBRAM-1A null mutant showed a genetic interaction with *daf-7* TGF-β pathway mutants and suppressed Daf-c phenotype, suggesting that CeBRAM-1A negatively regulates this pathway. *CeBRAM-2B::GFP* was expressed in pharyngeal muscle and intestinal cells. Loss-

of function of CeBRAM-2B by double strand RNA interference (dsRNAi) (Montgomery et al., 1998; Fire et al., 1998) resulted in worms with Lon phenotype, suggesting that CeBRAM-2B is a negative regulator of the *sma* pathway. Together, these results strongly suggest that the two related molecule CeBRAM-1A and CeBRAM-2B are negative regulators of the *daf* pathway and the *sma* pathway, respectively, and define a novel family of proteins, in the nematode *C. elegans*.

III-3 Results

Isolation and characterization of CeBRAM-1A and CeBRAM-2B cDNA.

To understand the signaling systems of the TGF-β superfamily in more detail, we have recently screened for BMP receptor associated molecules by the yeast two-hybrid screening system. we isolated a human gene encoding a protein that binds to BMP receptor type I (BMPRI/ALK3), and designated it as BMP receptor associated molecule-1 (BRAM-1) (Kurozumi et al., 1998). hBRAM-1 was found to be an alternatively-spliced form of BS69, a previously-identified adenovirus E1A-associated protein (Hateboer 1995). Although the cytoplasmic protein BRAM-1 has been shown to bind specifically to BMPRI-A, *in vivo* function was not clear.

By searching a *C. elegans* DataBase (ACeDB), it was found that two genes which are similar to human BRAM-1 are present in *C. elegans* genome. They were tentatively named as CeBRAM-1A and CeBRAM-2B, respectively. In this study, I investigated the function of CeBRAM-1A and CeBRAM-2B. CeBRAM-1A was mapped to F54B11. 1 on chromosome X (Figure 3-1 B) but no mutants were found in this region. This clone contains a single open reading frame of 888 nucleotides. Predicted CeBRAM-1A protein consists of 183 amino acids (Figure 3-1 A). CeBRAM-2B was mapped to F23H11.1 on the left arms of chromosome III (Figure 3-2 B) but again, no mutants were found in this region. This clone contains a single open reading frame of 909 nucleotides. Predicted CeBRAM-2B protein consists of 214 amino acids (Figure 3-2 A). Comparison of predicted CeBRAM-1A amino acid sequence with hBRAM-1 revealed an overall identity of 27% with a divergent amino terminal domain (20% identity) followed by a closely related 64-residue carboxy-terminal domain (45% identity) (Figure 3-3B). Comparison of CeBRAM-2B amino acid sequence with hBRAM-1 revealed an overall identity of 25% with a divergent amino terminal domain (19% identity)

followed by a closely related 69-residue carboxy-terminal domain (40% identity) (Figure 3-3B). In the case of CeBRAM-1A with CeBRAM-2B (Figure 3-3C), an overall identity is 53% with a divergent amino terminal domain (45% identity) followed by a closely related 69-residue carboxy-terminal domein (70% identity).

CeBRAM-1A shares identical amino acids with human BRAM-1 particularly in C-terminal region (Figure 3-3A). However, a higher molecular weight form corresponding to mammalian BS69 is unlikely to be present in *C. elegans*, because Northern blot analysis of mRNA from mixed stage of *C. elegans* gave a single band of approximately 800 bp and which represents a full length of CeBRAM-1A transcript. Same result was obtained by the Northern blot analysis of CeBRAM-2B.

C-terminal domain of CeBRAM-1A and CeBRAM-2B are conserved from *C. elegans* to human.

By searching GenBank, I found a protein, human RACK7, which has a conserved domain of C-terminal regions of CeBRAM-1A, CeBRAM-2B and human BRAM-1. RACK7 was identified as protein kinase C (pkC) -binding protein (unpublished), but its function has not been elucidated. Figure 3-3A shows the amino acid comparison of CeBRAM-1A, CeBRAM-2B human BRAM-1 with RACK7 (200-400 residues). Comparison of predicted RACK7 amino acid sequence with hBRAM-1 revealed an overall identity of 17% with a divergent amino terminal domain (17% identity) followed by a closely related 64-residue carboxy-terminal domein (40% identity) (Figure 3-3B). The conserved regions have two stretches of consensus amino acid residues, KKQWCXXCXXEA and CCWNTXYCXXXCQQXHW, and both motifs are predicted to be a zinc-finger related domain which is important for protein-DNA, or protein-protein interaction (Figure 3-3A). With these conserved domains, I searched GenBank and ACeDB. But another related protein which has this domain has not been found in the database. Because the C-terminal half of human BRAM-1 was shown to be sufficient for binding to BMP receptor-1A (Kurozumi et al.), these conserved predicted zinc-finger domains seem to be necessary for association to type I receptor (Figure 3-5; Kurozumi et al 1998).

***CeBRAM-1A::GFP*is expressed in neurons.**

To examine the expression pattern of CeBRAM-1A, transgenic animals

carrying green fluorescent protein (GFP) reporter construct (*CeBRAM-1A::GFP*) were generated. *CeBRAM-1A::GFP* was expressed strongly in amphid and phasmid neurons, and weak expression was observed in the hypodermal cells and ventral nerve cord (VNC) (Figure 3-4B). This expression pattern was consistent through larval to adulthood. Identified neurons include AWC, AFD, ASI, ASG, ASK, ASJ amphid neurons (Figure 3-4C, D) and PHA and PHB pasmid neurons (Figure 3-4D, F). This expression pattern was similar to that of DAF-1. As shown previously by a laser cell ablation experiment, ADF, ASI, and ASG are responsible for the signal to inhibit dauer formation and ASJ for the signal to exit from the dauer stage (Bargmann and Horvitz 1991). DAF-7, the ligand of the *daf* pathway is expressed in amphid neuron ASI and thought to be act like as a neurotransmitter (Ren et al., 1996; Schackwitz et al., 1996). The localized expression of CeBRAM-1A in ASI, ASG and ASJ suggested that CeBRAM-1A is involved in the regulation of dauer larva formation.

***CeBRAM-2B::GFP* is expressed strongly in pharyngeal muscle and intestinal cells and weak expressions were seen in neurons.**

To examine the expression pattern of CeBRAM-2B *in vivo* at cellular level, we generated transgenic worms expressing a *CeBRAM-2B::GFP*fusion gene. Strong GFP expressions were observed in the pharyngeal muscle of the anterior and posterior bulbs of the pharynx (Figure 3-5A) and posterior region of the intestinal cells (Figure 3-5B). This expression profile was consistent through L1 to adulthood. It is intriguing to note that this expression pattern of CeBRAM-2B is similar to that of *sma-6* receptor acting in the *sma* pathway which is also expressed in pharyngeal muscle and in the intestinal cells (Krishna et al., 1999). These results indicate that CeBRAM-2B functions in the same cells of *sma-6* type I receptor. Weak expressions were seen in ventral nerve cord (VNC) (Figure 3-5A), where *CeBRAM-1A::GFP*was also expressed. This result indicates the possibility that some functional redundancy is present between CeBRAM-1A and CeBRAM-2B.

CeBRAM-1A associates with DAF-1 type I receptor

Because the C-terminal half of human BRAM-1 was shown to be sufficient for association with BMP receptor-1A (Kurozumi et al., 1998), it was expected that vertebrate BRAM-1 and CeBRAM-1A shares a common function in

receptor-binding thereby participating in TGF-β pathway in vertebrate and *C. elegans*, respectively. Also, the expression pattern of *CeBRAM-1A::gfp* fusion was resembling that of DAF-1 type I receptor (Figure 3-4), it is expected that CeBRAM-1A is involved in the *daf* signaling pathway. To confirm this, I first performed a glutathione S-transferase (GST) pull-down assay using mammalian COS7 cells transiently transfected with cDNAs of hemagglutinin (HA)-CeBRAM-1A and GST-DAF-1 or GST-BMPR-IA (Figure 3-6). GST-DAF-1 as well as GST-BMPR-IA fusion proteins were efficiently immunoprecipitated with anti-HA antibody, through the binding to HA-tagged CeBRAM-1A. The result suggests that CeBRAM-1A physically interacts not only with the DAF-1 type-1 receptor but also with the mammalian BMP receptor-1A *in vivo* (Figure 3-6). Further analysis of binding specificity of CeBRAM-1A to other type I receptor such as *sma-6*, and CeBRAM-2B with DAF-1 or SMA-6, remains to be coming out.

Isolation and characterization of CeBRAM-1A null mutants

To investigate the functional role of CeBRAM-1A, I utilized the strategy of gene disruption by insertion of a Tc1 transposable element in the CeBRAM-1A genomic region. Subsequent excision and transposition of Tc1 would likely to result in a deletion of the functional domains of the targeted gene (Zwaal et al., 1993). I screened pools of potential mutants for successful insertion of the Tc1 transposon in the region of CeBRAM-1A gene by polymerase chain reaction (PCR) using specific oligonucleotide primers. Figure 3-7 shows one case in which Tc1 was inserted into the intron between third and fourth exons (Figure 3-7A). I, then, screened for worms in which transposition of Tc1 caused deletions that might affect the function of CeBRAM-1A. As a result, I identified one mutant allele, *kk1*, that deleted 816 bp of CeBRAM-1A coding region (Figure 3-7B). It is believed that *kk1* is a null mutation because the entire region that covers exon 1 to exon 3 of CeBRAM-1A was deleted and this deletion was expected to cause no functional translated product (Figure 3-7B). The mutant of CeBRAM-1A *(kk1)* showed a head-lifting phenotype, typical phenotype seen in mutants such as *cat-2* (catecholamine abnormality) whose dopamine level is significantly reduced (Loer and Kenyon 1993). Other abnormality was not detected by external observation.

Genetic interaction of CeBRAM-1A and *daf-7* TGF-β signaling mutants.

To investigate the involvement of CeBRAM-1A to the *daf-7* TGF-β pathway, I generated double mutant of CeBRAM-1A *(kk1)* with *daf-1*, a dauer constitutive (*daf-c*) mutant. In temperature-sensitive alleles of *daf-1* mutation, *m 40, m 402, m 213*, a large fraction of the mutant worms spontaneously transform into dauer larva at 20℃ and all worms undergo dauer formation at 25℃. However, the dauer larva was significantly reduced in double mutants of *daf-1* or *daf-7* and *kk1* (Table 3-1). The result showing loss of function of CeBRAM-1A suppressed the *daf-7* and *daf-1* phenotype suggests that CeBRAM-1A acts as a negative regulator of the *daf-c* pathway which consists of TGF-β signaling components. Because *daf-7* and *daf-1* is encoding a ligand and type I receptor responsible for *daf-c* signal, respectively, CeBRAM-1A is suggested to act downstream of the ligand and receptor. Dauer larva formation of double mutant of *kk1* and *daf-11(m 52)*, which acts upstream of the ligand and receptor was also significantly reduced. By contrast, double mutant with *daf-14* that is encoding a SMAD family of protein which is supposed to act downstream of the ligand and the receptor, showed no obvious change in efficiency of dauer larva formation. Together, it is strongly suggested that CeBRAM-1A acts between DAF-1 type I receptor and DAF-14 SMAD protein. The repression of the temperature-sensitive dauer formation in the *kk1* mutant was recovered by the transgene of genomic fragment of CeBRAM-1A region.

Double strand RNA interference (dsRNAi) of CeBRAM-2B caused Lon phenotype.

To investigate the functional role of CeBRAM-2B, I utilized the recently developed strategy of gene disruption by double strand RNA-mediated genetic interference (dsRNAi). dsRNAi that uses double stranded RNA of several hundred basepairs, is currently used to disrupt gene activity not only in the nematode, but also in the fly. (Fire et al., 1998; Montgomelly et al., 1998; Kennerdell et al 1999). dsRNA injected into adult hermaphrodite gonad, specifically blocks gene activity by unknown mechanism. The effects of interference were observed in the injected worms and their progeny. I used dsRNA corresponding to CeBRAM-1A and CeBRAM-2B. The dsRNAi of CeBRAM-2B showed Lon phenotype (Figure 3-8B). When the mixture of dsRNAs of CeBRAM-1A and CeBRAM-2B (CeBRAMs) were injected, frequency of Lon

phenotype increased (Figure 3-8C). dsRNAi of CeBRAM-1A alone did not cause Lon phenotype (Figure 3-8D). Previously, I showed that overexpression of *cet-1* in N2 wild type animal caused Lon phenotype. Furthermore *cet-1* regulates *C. elegans* body length in a dose dependent manner (see part I). Thus, Lon phenotype seems to be activated state of the *cet-1/sma* pathway signaling. These results suggest the possibility that CeBRAM-2B is involved dominantly in the *cet-1/sma* pathway and negatively regulate this pathway like CeBRAM-1A in the *daf* pathway.

Isolation and characterization of CeBRAM-2B null mutants.

To confirm the result of dsRNAi of CeBRAM-2B, I screened CeBRAM-2B null mutant by chemical mutagenesis, TMP-UV method (Yandell et al., 1994). I screened 600 plates which contain almost 3×10^5 genomes of potential mutants for successful deletion of chemical mutagenesis by TMP-UV in the region of CeBRAM-2B gene by polymerase chain reaction (PCR) using gene specific oligonucleotide primers. I isolated one deletion allele, *kk5*. Because *kk5* had a deletion of a 1418 bp that covers entire second and third exons of CeBRAM-2B which is thought to be essential for function of CeBRAM-2B product, CeBRAM-2B*(kk5)* is expected to be a null or strong loss-of-function allele (Figure 3-9). However, phenotype of the mutant *kk5* is not clear at this moment and further back-cross against N2 wild type to clean up the genome is required to determine the conclusive phenotype.

III-4 Discussion

CeBRAM-1A may be a negative regulator of the *daf-7* TGF-β pathway.

Recent studies on TGF-β signaling pathway in *C. elegans* have revealed that there are at least two distinct TGF-β pathways that regulate neuronal activities and body length of the nematode, respectively. In this study, I have demonstrated that CeBRAM-1A is encoding a homologue of human BRAM-1 which was identified as a BMP receptor associated protein. Based on the expression of *CeBRAM-1A::GFP*, CeBRAM-1A seems to be expressed in the amphid and phasmid neurons (Figure 3-4) and this expression pattern is similar to that of *daf-1* which is encoding type I receptor of the *daf* pathway in *C. elegans*

(Georgi et al., 1991). I also showed that CeBRAM-1A can bind to DAF-1 type I receptor by GST-pull down assay (Figure 3-6). These results indicate that CeBRAM-1A may act in the same cells in which*daf-1* receptor is functioning. Finally, I isolated CeBRAM-1A null mutant by Tc1 deletion method. Genetic analysis of CeBRAM-1A null mutant with *daf-7* TGF-β pathway component mutants revealed that CeBRAM-1A suppressed the *daf-c* phenotype if it was partially (Table 3-1). These results strongly suggest that CeBRAM-1A is a negative regulator of the *daf-7* TGF-β signaling pathway in *C. elegans*.

DAF-7, the ligand in the *daf* pathway, is expressed in the ASI amphid neuron and is thought to act in a neuroendocrine manner, regulating developmental and metabolic shifts in tissues that are remodeled during dauer formation. (Ren et al., 1996; Schackwitz et al., 1996). Here, I demonstrate that CeBRAM-1A is expressed in the neurons including ASI neurons where *daf-1* is also expressed. Therefore, it is likely that dauer larva formation is regulated by interneuronal communications between DAF-7-producing ASI and other neurons expressing DAF-1 and CeBRAM-1A near by ASI.

I showed that CeBRAM-1A null mutant not only suppressed Daf-c phenotype, but also displayed head-lifting phenotype. The *daf-7* TGF-β pathway mutants do not have the head-lifting phenotype. This is the typical phenotype seen in mutants such as *cat-2* (catecholamine abnormality) whose dopamine level is significantly reduced (Loer and Kenyon 1993). This suggests that CeBRAM-1A may have additional functional roles related to neuronal activity.

CeBRAM-2B may be a signal mediator of the *cet-1/sma* TGF-β pathway and function as a negative regulator of this pathway.

I demonstrate that CeBRAM-2B is another homologue of human BRAM-1 in *C. elegans*. *CeBRAM-2B::GFP* is expressed mainly in pharyngeal muscle and intestinal cells (Figure 3-5). These expression pattern is similar to that of *sma-6* which is encoding the type I receptor of the *sma* pathway in *C. elegans*.

dsRNAi of CeBRAM-2B caused Lon phenotype (Figure 3-8). This indicate that loss-of function of CeBRAM-2B gene causes Lon phenotype. I showed previously that activation of the genes of the *cet-1/sma* pathway caused Lon phenotype. To conclude the function of CeBRAM-2B, I should show that CeBRAM-2B functions in the *cet-1/sma* pathway by genetic analysis making

double mutant of CeBRAM-2B loss-of-function mutant with the *cet-1/sma* pathway mutants.

I showed that dsRNAi using the mixture of CeBRAM-1A and CeBRAM-2B dsRNAs enhanced the Lon phenotype compared with the result of dsRNAi of CeBRAM-2B alone (Figure 3-8). These results suggest that some functional redundancy is present between the function of CeBRAM-1A and CeBRAM-2B. The observation that expression patterns of *CeBRAM-1A::GFP* and *CeBRAM-2B::GFP* overlap in several regions for example VNC, hypodermis, and intestinal cells (Figure 3-4, 5), supports the presence of some functional redundancy of these genes. CeBRAM-2B dominantly contribute the *cet-1/sma* pathway, because, dsRNAi of CeBRAM-1A alone did not cause Lon phenotype at all. To confirm these result, more analysis should be done by the genetic interaction of CeBRAM-1A null mutant *(kk-1)*, with CeBRAM-2B loss-of-function mutants.

CeBRAM-1A and CeBRAM-2B are conserved proteins in invertebrate as well as in vertebrate and defines a family of related protein.

I identified two homologue of the human BRAM-1 in *C. elegans*. These genes have extremely conserved C-terminal region (Figure 3-3). These region have two consensus sequences which seems to be a zinc-finger related domain. The zinc-finger domain is known to be important for interaction of protein not only with DNA, but also with protein. Because the C-terminal half of human BRAM-1 was shown to be sufficient for binding to BMP receptor-1A (Kurozumi et al.), this conserved predicted zinc-finger domain seems to be necessary for association of BRAMs to type I receptor.

I also found another gene that has this conserved region, RACK7, which has reported as a PKC binding protein. However, the function of RACK7 is not clear. Nevertheless, these results indicate that BRAM-1 related proteins define a new class of family proteins.

Upon completion of the *C. elegans* genome project, we know almost all the structure of genes in *C. elegans*. In *C. elegans* TGF-β type I receptor related genes are found only two, which are *daf-1* (Estevez et al., 1993) and *sma-6* (Krishuna et al., 1999). BRAM-1 related genes which I found in *C. elegans* genome are also two, : CeBRAM-1A and CeBRAM-2B. This may suggest that each type I receptor has one pathway-specific BRAM-1 related molecule to associate with it and to be negatively regulated.

Possible mechanism of negative regulation of TGF-β signaling pathway by CeBRAM-1A and CeBRAM-2B.

In the TGF-β signaling system, association and phosphorylation of pathway-restricted Smads by the type I receptor is essential for activating the TGF-β signaling pathway (Heldin et al., 1997). However, little is known how Smad interaction with receptor is controlled. Here, I described the identification of novel type I receptor associated proteins CeBRAM-1A and CeBRAM-2B in *C. elegans*. Genetic analysis of CeBRAM-1A null mutant with previously known *daf-7* TGF-β pathway mutants revealed that CeBRAM-1A is epistatic to *daf-7* and *daf-1*, and hypostatic to *daf-14* (Table 3-1). Because *daf-7*, *daf-1*, and *daf-14* are encoding ligand, type I receptor and SMAD proteins, respectively, CeBRAM-1A may be acting between type I receptor and the SMAD protein and negatively regulate this pathway in *C. elegans*. I also demonstrate that CeBRAM-1A associates with DAF-1 type I receptor (Figure 3-6). Taken together with these results, I propose a hypothesis for negative effect of CeBRAMs to TGF-β signaling pathways that CeBRAMs blocks the physical interaction of type I receptor and SMAD proteins (Figure 3-10). To confirm this possibility, further analysis on protein-protein interaction is required.

Recently, a Smad2 binding protein, SARA, was identified (Tsukazaki et al., 1999). SARA recruits Smad2 into distinct subcellular domains and that SARA colocalizes and interacts with TGF-β receptors. TGF-β signaling induces dissociation of Smad2 from SARA with concomitant formation of Smad2/Smad4 complexes and nuclear translocation. Thus, SARA defines a component of TGF-β signaling that functions to recruit Smad2 to the receptor by controlling the subcellular localization of the Smad. SARA interacts with the TGF-β receptor independently of Smad2 binding and that Smad2 cooperates to enhance association. SARA also defines a family of related proteins (Tsukazaki et al., 1999). In addition to SARA, CeBRAMs may also represent a new class of TGF-β family signal mediator proteins.

Concluding Remarks

Regulation of the size of animal development.

Members of the TGF-β superfamily regulate many aspect of cell growth and differentiation in a variety of animal species. In *C. elegans*, I identified a novel TGF-β-like ligand, *cet-1*. By means of deletion mutations and overexpression analysis, I showed that CET-1 regulates the *C. elegans* body length in a dose dependent manner. This result seems to contain some answers of the general question how the size of an animal or plant is determined (reviewed by Conlon et al., 1999), which is one of the most fundamental question of animal development. The size of an animal depends on the number and size of the cells it contains as well as on the amount of extracellular matrix and fluid. In *C. elegans*, I showed that the regulation of body length by *cet-1* seems to depend not on the cell-number but on the cell-volume. But, the exact molecular mechanism by which body length and cell size regulation is determined remains to be solved.

To elucidate the mechanism how body length is determined by *cet-1*, I am now screening additional downstream target genes which are regulated by *cet-1*. Previous studies on the epistatic relationships between *sma* genes and *lon* genes placed *lon-2* upstream of the *cet-1/sma* components in the same pathway. Using *lon-2* mutant which seems to be up-regulated the *cet-1/sma* pathway, N2 wild type, and *cet-1* null mutant, I have recently performed differential hybridization screening with high-density filters, on which over 7,000 independent *C. elegans* cDNAs provided by Dr. Kohara were arrayed. We isolated mRNAs from synchronized L3 larvaes of N2, *cet-1* and *lon-2*, respectively, and then cDNAs labeled with ^{32}P, were synthesized and hybridized to the arrayed filters. By comparing the intensity of hybridization to replicas of the cDNA set with probes prepared from N2, *cet-1* and *lon-2* mutants, I identified several genes whose expression was changed by the loss or gain of *cet-1* signaling. In the near future, this approach will provide us useful information about how *cet-1* regulates *C. elegans* body length.

Modulator of the TGF-β signaling.

TGF-β family members regulate the broad range of cellular functions. These multifunctional effect of TGF-β family ligands are restrictively controlled

by binding to its extracellular antagonists and cross-talking with another signaling pathways. BMP signal is controlled by its antagonistic modulator proteins, chordin, noggin and follistatin extracellularly (Zimmerman et al., 1996; Piccoro et al., 1996; Iemura et al., 1998). These antagonist associate directly with the BMP ligand, and modulate the effective region of the ligands. The intracellular control is also important. Cytoplasmic protein, SARA, has been shown to regulate the cellular localization of SMAD protein, and controls the signaling of TGF-β (Tsukazaki et al., 1998). Some cross-talks have been reported between TGF-β/SMAD signaling and interferon-γ/STAT pathway by the transmodulation of intracellular signal components intracellularly (Ulloa et al., 1999). These complex regulations of the signaling of TGF-β family may lead to the complex out put of the ligands. I demonstrated that the identification of new signal mediators of TGF-β signaling, CeBRAM-1A and CeBRAM-2B, both of which associate with type I receptors. By means of loss-of-function analysis and genetic interaction tests, I showed that CeBRAM-1A and CeBRAM-2B negatively regulate the *daf* and the *sma* TGF-β pathways, respectively, in *C. elegans*. In addition, CeBRAMs-related proteins appears to be conserved from human to the nematode and define a new class of family proteins. The precise mechanism of negative regulation is not fully understood. However, I hope that results in this study will provide a new aspect to the regulational mechanism of TGF-β signaling system.

V Materials and Methods

General methods and strains in part I

C.elegans strains were cultured as described by Brenner (1974) and grown at 20℃ unless otherwise noted. Genetic cross were performed as described by Wood (1988). The following strains were used in this work: wild type *C.elegans* variety Bristol strain (N2), *daf-4(m63)III, daf-7(m62)III, daf-7(e1372)III, sma-2(e502)III, sma-3(e491)III, sma-4(e729)III, lon-1(e185)III, mab-21(bx53)III; him-5(e1490), him-5(e1467)V, dpy-11(e224); unc-42(e270)V, unc-46(e177); dpy-11(e224)V, him-5(e1490); wxIs11, him-5(e1490); wxIs22, sma-6(wk7)IV; him-5(e1492)V.*

Isolation of *cet-1* cDNA

A set of degenerate oligonucreotide primers were designed to target conserved sequences present in the subfamily of TGF-β members including BMPs, Vg-1, and *dpp* (Basler et al., 1993). The forward polymerase chain reaction (PCR) primer was 5'TGG(AG)A(AT)GA(CT)TGGAT(AT)(AG)T(AT)GC-3'; the reverse PCR primer was 5'-GT(CT)TG(GT)A(CT)(AG)AT(AGT)GC(AG)TG(GT)TT-3'. These two primers were used in PCR for 40 cycles at 94° C for 1 min, 50° C for 1 min, 72° C for 1.5 min using *C. elegans* total cDNA as a template. The amplified PCR products were subcloned into pBluescript II KS- and sequenced by dideoxy chain-termination method with BcaBest (TAKARA). One of the 0.11-kb clones was used to screen a mixed stage *C. elegans* cDNA library to obtain a full-length clone.

Phylogenetic tree

Sequence alignment and construction of phylogenetic tree were performed by GENETIX-MAC software (SOFTWARE DEVELOPMENT CO., LTD). These results were confirmed by alignment with Pileup (GCG software), making distance tree by the method with Jukes-Cantor Distance and Kimura Two - Parameter Distance.

Germline transformation of *C. elegans*

Microinjection of DNAs into the gonadal syncytia of *C. elegans* hermaphrodites was carried out as described previously (Mello et al., 1991). Each transformation result was scored with multiple independent transgenic lines. All

plasmids were injected at a concentration of 100 ng/μl. For GFP-expression, a translational *cet-1::GFP* fusion containing a nuclear localization signal was made by cloning the 4.1-kb *Sph*I-*Sal*I fragment derived from the cosmid T25F10 into the *Sph*I-*Sal*I site of pPD95.69 (gifted from A. Fire) and named pA05. For transformation, a 10:1 mixture of pA05 and pJM23 carrying *lin-15(+)* gene (Huang et al., 1994) was injected into *lin-15(n765)* hermaphrodites at a total concentration of 100 ng/μl. Non-Lin worms with normal vulvas grown at 25℃ were selected as transgenic animals. For rescue and overexpression experiments, a 9.3 kb *Apa*I-*Pst*-1 fragment of T25F10 was subcloned into pBluescript SK- and named pA07. A high concentration(10:1) mixture of pA07 and pGFP-myo3 and low concentration(100:1) mixture were injected into N2, *cet-1(kk3)* and *lon-1(e185)*. GFP expression was used to select for transgenic worms.

Isolation of *cet-1* null mutant

Transposable elements were targeted using a PCR and sib-selection scheme performed as described by Zwaal et al., 1993. Insertions were visualized by using nested PCR. The position of the Tc1 insertions were confirmed by multiple PCR reactions with flanking primers, followed by direct sequencing of the PCR products from both insertion junctions. Subsequently, Tc1 specific primers, Tc102 5′-AGCCAGCTACAATGGCTTTC-3′, Tc103 5′-GATGCAAACGGATACGCGAC-3′, Tc104 5′-CCAAACAAATCCAGTGCAAC-3′, Tc105 5′-TGTCATTTCCTTGCAACCTC-3′, and gene-specific primers MS7 '5-CATGGACAAACATCGGGGA-3′, MS8 5′-AGGAACATTAGGAAGGAATCA-3′, MS11 5′-CGTGTACACAAATCTGTTCG-3′, MS12 5′-CGATTCTCGAGGTGGTCTCA-3′, MS15 5′-GATATTCGATACGGAGACGG-3′, MS16 5′-ACTCGCAACTTCAAGAATGT-3′ were used. To isolate the Tc1 insertion mutant, next primer sets were used, Tc 102, 103, 104, 105, and MS 11, 12. To isolate the deletion allele, *kk3*, MS7, 8, 11, 12 were used. In this case, no visible band was seen with no deletion, and visible band has been amplified, when deletion was introduced. To isolate the deletion allele, *kk4*, MS11, 12, 15, 16 were used. After isolation of the deletion mutants, they were backcrossed against N2 wild type animals 10 times, and after that, crossed with *dpy-11(e224); unc-42(e270)V* and *unc-46(e177); dpy-11(e224)V* respectively, to clean up chromosome V.

Body length measurement of adult mutant worms

Animals were grown at 20° C. Newly laid embryos were collected over a 3-5 hr time period. 5 days later, F1 adult animals which were distinguishable from F2 animals, were transferred to a new plate and anesthetized with 200 µl of 10 mM sodium azide solution for 5 min. Anesthetized animals were linearized and their body lengths measured with dissecting microscopy and micrometer.

Dauer formation phenotype counts

The frequency of dauer formation was assessed under noninducing conditions essentially as described by Thomas et al., 1993. Noninducing conditions were defined as uncrowded animals on well seeded 6-cm NG agar plates. Between 4 and 12 adult hermaphrodites were placed on a plate at the test temperature. After allowing egg laying for a limited time (less than 12 hr at 25° C) the parents were removed. As the progeny matured, the plates were checked frequently and L4 nondauers were counted and removed to prevent a new generation of eggs.

Strains and genetics of the study of part II

The techniques used for culturing *C.elegans* were essentially as described by Brennner (1974) and were grown at 20℃ unless noted otherwise.

The following strains were used in Part 2.: wild type *C.elegans* variety Bristol strain (N2), *daf-1(m 402)IV*, *daf-1(m 213)IV*, *daf-1(m 40)IV*, *daf-7(m 62)III*, *daf-7(e1372)III*, *daf-11(m 47)V*, *daf-14(m 77)IV*, *mut-2(r459)I; dpy-19(n1347)III*, *dpy-9(e12)IV*, *unc-42(e270)V*, *unc-43(e408)IV*, *unc-45(e286)III*,

Generation of CeBRAM-1A and CeBRAM-2B expression constructs

2 kb fragments including upstream regulatory sequences and CeBRAM-1A or CeBRAM-2B cordig region were amprified by PCR and were used to generate a translational fusion containing a nuclear localization signal or not with the GFP gene in the vector pPD95.67 (courtesy of A. Fire).

Isolation of Tc1 insertions in CeBRAM-1A and deletion derivatives

Transposable elements were targeted using a PCR and sib-selection scheme performed. Insertions were visualized by using nested PCR. The position of the Tc1 insertions were confirmed by multiple PCR reactions with flanking

primers, followed by direct sequencing of the PCR products from both insertion junctions. Subsequently, Tc1 specific primers, Tc102 5'-AGCCAGCTACAATGGCTTTC-3', Tc103 5'-GATGCAAACGGATACGCGAC-3', Tc104 5'-CCAAACAAATCCAGTGCAAC-3', Tc105 5'-TGTCATTTCCTTGCAACCTC-3', and gene-specific primers CBM-1 (5'-GGCTCATGACCACATATCGA-3'), CBM-2 (5'-ACTCGCCTCATGGGCTCATT-3'), CBM-3 (5'-GATCTCTCCGAAATTGATCC-3'), CBM-4(5'-TCTCGAAGGAATTAACACAAGT-3') were used. After isolation of the deletion mutants, they were backcrossed against N2 wild type animals 10 times.

Construction of CeBRAM-1A; *daf-c* double mutants

Construction of double mutants were performed using recessive visible trans markers tightly linked to the *daf-c* mutation. An example is the construction of *daf-1;* CeBRAM-1A mutant. CeBRAM-1A is on chromosome X, while *daf-1* and *dpy-9* are tightly linked on chromosome VI. First, *dpy-9;* CeBRAM-2 mutant were constructed. *dpy-9/+* males were mated to CeBRAM-2 hermaphrodites and the F2 dpy progeny were picked singly to plate. CeBRAM-1A genotype was checked by using PCR. Next, *daf-1* males were mated to *dpy-9;* CeBRAM-1A hermaphrodites and F2 non-dpy progeny were picked singly to plate. CeBRAM-1A genotype was checked by using PCR. The plate of non-dpy progeny was *daf-1;* CeBRAM-1A double mutants.

Dauer formation phenotype counts

The frequency of dauer formation was assessed under noninducing conditions essentially as described by Thomas et al., 1993. Noninducing conditions were defined as uncrowded animals on well seeded 6-cm NG agar plates. Between 4 and 12 adult hermaphrodites were placed on a plate at the test temperature. After allowing egg laying for a limited time (less than 12 hr at 25° C) the parents were removed. As the progeny matured, the plates were checked frequently and L4 nondauers were counted and removed to prevent a new generation of eggs.

dsRNAi (double strand RNA interference) of CeBRAM-2B

The templates used for synthesis of RNAs were cDNA clones of

CeBRAM-1A, CeBRAM-2B of YK clone (gifted by Y. Kohara). Plasmids were linearized by appropriate restriction enzymes. RNA synthesis was done by Megascript Kit (invitrogen) with T3, and T7 primers. After the reaction, each fraction were mixed and maintained at 65° C for 10 min and annealed with each other at 37° C for 30 min. Synthesized double strand RNA was injected to the gonadal syncytia of adult hermaphrodites. F1 progenys were analyzed of their phenotype.

Isolation of CeBRAM-2B null mutant by TMP-UV methods

To identify the CeBRAM-2B null mutant, we performed chemical mutagenesis by TMP-UV method (Yandel et al., 1994). Synchronized L4 animals were treated with 3 mg/ml TMP (4, 5, 8-trimethyl psoralen), and irradiated with 365 nm UV for 340 W /cm for 60 sec. F1 animals were cultured 6 cm NGM plates (600 plates) with approximately 500 animals with each plates. After starvation, the worms were washed and harvested with 3 ml H_2O. After lysis, the presence of deletions were checked by two rounds of a selective PCR, using pairs of CeBRAM-2B gene specific nested primers. Specific primers, CBM-15 (5'-GAGCCAAGAAGCGGTTGAAA-3'), CBM-16 (5'-GGTTATTCAAGTAGTGTCGG-3'), CBM-17 (5'-TTCATGAGACTTTCTGGCGC-3'), CBM-18 (5'-GGTAACCAAAGTGTCCTTGT-3') were used. Two round sibling selection was done.

Reference

Albert, P. S., Brown, S. J., and Riddle, D. L. (1981). Sensory control of dauer larva formation in Caenorhabditis elegans. *J Comp Neurol* 198, 435-51.

Baird, S. E., and Emmons, S. W. (1990). Properties of a class of genes required for ray morphogenesis in Caenorhabditis elegans. *Genetics* 126, 335-44.

Baird, S. E., Fitch, D. H., Kassem, I. A., and Emmons, S. W. (1991). Pattern formation in the nematode epidermis: determination of the arrangement of peripheral sense organs in the C. elegans male tail. *Development* 113, 515-26.

Bargmann, C. I., and Horvitz, H. R. (1991). Control of larval development by chemosensory neurons in Caenorhabditis elegans. *Science* 251, 1243-6.

Basler, K., Edlund, T., Jessell, T. M., and Yamada, T. (1993). Control of cell pattern in the neural tube: regulation of cell differentiation by dorsalin-1, a novel TGF beta family member. *Cell* 73, 687-702.

Brenner, S. (1974). The genetics of Caenorhabditis elegans. *Genetics* 77, 269-271

Chen, X., Rubock, M. J., and Whitman, M. (1996). A transcriptional partner for MAD proteins in TGF-beta signalling *Nature* 383, 691-6.

Chen, X., Weisberg, E., Fridmacher, V., Watanabe, M., Naco, G., and Whitman, M. (1997). Smad4 and FAST-1 in the assembly of activin-responsive factor. *Nature* 389, 85-9.

Chow, K. L., and Emmons, S. W. (1994). HOM-C/Hox genes and four interacting loci determine the morphogenetic properties of single cells in the nematode male tail. *Development* 120, 2579-92.

Chow, K. L., Hall, D. H., and Emmons, S. W. (1995). The mab-21 gene of Caenorhabditis elegans encodes a novel protein required for choice of alternate cell fates. *Development* 121, 3615-26.

Colavita, A., Krishna, S., Zheng, H., Padgett, R. W., and Culotti, J. G. (1998). Pioneer axon guidance by UNC-129, a C. elegans TGF-β. *Science* 281, 706-9

Conlon, I., and Raff, M. (1999). Size control in animal development. Cell 235-44.

Cowing, D., and Kenyon, C. (1996). Correct Hox gene expression established independently of position in Caenorhabditis elegans. *Nature* 382, 353-6.

Dubois, C. M., Laprise, M. H., Blanchette, F., Gentry, L. E., and Leduc, R. (1995). Processing of transforming growth factor beta 1 precursor by human furin convertase. *J Biol Chem* 270, 10618-24.

Emmons, S. E. (1998). Cell fate determination in C. elegans ray development. In: Cell Fate and Lineage Determination. *Moody, S.A. Ed. Academic Press.*

Estevez, M., Attisano, L., Wrana, J. L., Albert, P. S., Massague, J., and Riddle, D. L. (1993). The daf-4 gene encodes a bone morphogenetic protein receptor controlling C. elegans dauer larva development. *Nature* 365, 644-9.

Epstein, H. F., and Shakes, D. C., eds. (1995) Methods in cell biology, vol. 48, Chaenorhabditis elegans: Modern biological analysis of an organism. *Academic Press*, New York

Feng, X. H., Zhang, Y., Wu, R. Y., and Derynck, R. (1998). The tumorsuppressor Smad4/DPC4 and transcriptional adaptor CBP/p300 are coactivators for smad3 in TGF-beta-induced transcriptional activation. *Genes Dev* 12, 2153-63.

Fire, A., Xu, S., Montgomery, M. K., Kostas, S. A., Driver, S. E., and Mello, C. C. (1998). Potent and specific genetic interference by double-stranded RNA in Caenorhabditis elegans. *Nature* 391, 806-11.

Georgi, L. L., Albert, P. S., and Riddle, D. L. (1990). daf-1, a C. elegans gene controlling dauer larva development, encodes a novel receptor protein kinase. *Cell* 61, 635-45.

Golden, J. W., and Riddle, D. L. (1984). A pheromone-induced developmental switch in Caenorhabditis elegans: Temperature-sensitive mutants reveal a wild-type temperature-dependent process. *Proc Natl Acad Sci U S A* 81, 819-23.

Gurdon, J. B., Harger, P., Mitchell, A., and Lemaire, P. (1994). Activin signalling and response to a morphogen gradient. *Nature* 371, 487-92.

Hahn, S. A., Schutte, M., Hoque, A. T., Moskaluk, C. A., da Costa, L. T., Rozenblum, E., Weinstein, C. L., Fischer, A., Yeo, C. J., Hruban, R. H., and Kern, S. E. (1996). DPC4, a candidate tumor suppressor gene at human chromosome 18q21.1. *Science* 271, 350-3.

Hateboer, G., Gennissen, A., Ramos, Y. F., Kerkhoven, R. M., Sonntag-Buck, V., Stunnenberg, H. G., and Bernards, R. (1995). BS69, a novel adenovirus E1A-associated protein that inhibits E1A transactivation. *Embo J* 14, 3159-69.

Hayashi, H., Abdollah, S., Qiu, Y., Cai, J., Xu, Y. Y., Grinnell, B. W., Richardson, M. A., Topper, J. N., Gimbrone, M., Jr., Wrana, J. L., and Falb, D. (1997). The MAD-related protein Smad7 associates with the TGFbeta receptor and functions as an antagonist of TGFbeta signaling. *Cell* 89, 1165-73.

Heldin, C. H., Miyazono, K., and ten Dijke, P. (1997). TGF-beta signalling from cell membrane to nucleus through SMAD proteins. *Nature* 390, 465-71.

Hogan, B. L. (1996). Bone morphogenetic proteins: multifunctional regulators of vertebrate development. *Genes Dev* 10, 1580-94.

Huang, L. S., Tzou, P., and Sternberg, P. W. (1994). The lin-15 locus encodes two negative regulators of Caenorhabditis elegans vulval development. *Mol Biol Cell* 5, 395-411.

Huang, X. Y., and Hirsh, D. (1989). A second trans-spliced RNA leader sequence in the nematode Caenorhabditis elegans. *Proc Natl Acad Sci U S A* 86, 8640-4.

Huse, M., Chen, Y. G., Massague, J., and Kuriyan, J. (1999). Crystal structure of the cytoplasmic domain of the type I TGF beta receptor in complex with FKBP12. *Cell* 96, 425-36.

Iemura, S., Yamamoto, T. S., Takagi, C., Uchiyama, H., Natsume, T., Shimasaki, S., Sugino, H., and Ueno, N. (1998). Direct binding of follistatin to a complex of bone-morphogenetic protein and its receptor inhibits ventral and epidermal cell fates in early Xenopus embryo. Proc Natl Acad Sci U S A 95, 9337-42.

Imamura, T., Takase, M., Nishihara, A., Oeda, E., Hanai, J., Kawabata, M., and Miyazono, K. (1997). Smad6 inhibits signalling by the TGF-beta superfamily. *Nature* 389, 622-6.

Jernvall, J., Aberg, T., Kettunen, P., Keranen, S., and Thesleff, I. (1998). The life history of an embryonic signaling center: BMP-4 induces p21 and is associated with apoptosis in the mouse tooth enamel knot. *Development* 125, 161-9.

Johnstone, I. L., Shafi, Y., and Barry, J. D. (1992). Molecular analysis of mutations in the Caenorhabditis elegans collagen gene dpy-7. *Embo J* 11,3857-63.

Jones, C. M., Dale, L., Hogan, B. L., Wright, C. V., and Smith, J. C. (1996). Bone morphogenetic protein-4 (BMP-4) acts during gastrula stages to cause ventralization of Xenopus embryos. *Development* 122, 1545-54.

Kawabata, M., Imamura, T., Miyazono, K., Engel, M. E., and Moses, H. L. (1995). Interaction of the transforming growth factor-beta type I receptor with farnesyl-protein transferase-alpha. *J Biol Chem* 270, 29628-31.

Kennerdell, J. R., and Carthew, R. W. (1998). Use of dsRNA-mediated genetic interference to demonstrate that frizzled and frizzled 2 act in the wingless pathway. *Cell* 95, 1017-26.

Kim, J., Johnson, K., Chen, H. J., Carroll, S., and Laughon, A. (1997). Drosophila Mad binds to DNA and directly mediates activation of vestigial by Decapentaplegic. *Nature* 388, 304-8.

Kingsley, D. M. (1994). The TGF-beta superfamily: new members, new receptors, and new genetic tests of function in different organisms. *Genes Dev* 8, 133-46.

Kretzschmar, M., Liu, F., Hata, A., Doody, J., and Massague, J. (1997). The TGF-beta family mediator Smad1 is phosphorylated directly and activated functionally by the BMP receptor kinase. *Genes Dev* 11, 984-95.

Krishna, S., Maduzia, L. L., and Padgett, R. W. (1999). Specificity of TGFbeta signaling is conferred by distinct type I receptors and their associated SMAD proteins in Caenorhabditis elegans. *Development* 126, 251-60.

Kurozumi, K., Nishita, M., Yamaguchi, K., Fujita, T., Ueno, N., and Shibuya, H. (1998). BRAM1, a BMP receptor-associated molecule involved in BMP signalling. *Genes Cells* 3, 257-64.

Levy, A. D., Yang, J., and Kramer, J. M. (1993). Molecular and genetic analyses of the Caenorhabditis elegans dpy-2 and dpy-10 collagen genes: a variety of molecular alterations affect organismal morphology. *Mol Biol Cell* 4, 803-17.

Loer, C. M., and Kenyon, C. J. (1993). Serotonin-deficient mutants and male mating behavior in the nematode Caenorhabditis elegans. *J Neurosci* 13, 5407-17.

Margolis, R. L., Stine, O. C., McInnis, M. G., Ranen, N. G., Rubinsztein, D. C., Leggo, J., Brando, L. V., Kidwai, A. S., Loev, S. J., Breschel, T. S., Callahan, C., Simpson, S. G., DePaulo, J. R., McMahon, F. J., Jain, S., Paykel, E. S., Walsh, C., DeLisi, L. E., Crow, T. J., Torrey, E. F., Ashworth, R. G., Macke, J. P., Nathans, J., and Ross, C. A. (1996). cDNA cloning of a human homologue of the Caenorhabditis elegans cell fate-determining gene mab-21: expression, chromosomal localization and analysis of a highly polymorphic (CAG)n trinucleotide repeat. *Hum Mol Genet* 5, 607-16.

Massague, J. (1996). TGFbeta signaling: receptors, transducers, and Mad proteins. *Cell* 85, 947-50.

Mello, C. C., Kramer, J. M., Stinchcomb, D., and Ambros, V. (1991). Efficient gene transfer in C.elegans: extrachromosomal maintenance and integration of transforming sequences. *Embo J* 10, 3959-70.

Meno, C., Saijoh, Y., Fujii, H., Ikeda, M., Yokoyama, T., Yokoyama, M., Toyoda, Y., and Hamada, H (1996). Left-right asymmetric expression of the TGF beta-family member lefty in mouse embryos. *Nature* 381, 151-5.

Meno, C., Shimono, A., Saijoh, Y., Yashiro, K., Mochida, K., Ohishi, S., Noji, S., Kondoh, H., and Hamada, H. (1998). lefty-1 is required for left-right determination as a regulator of lefty-2 and nodal. *Cell* 94, 287-97.

Miya, T., Morita, K., Suzuki, A., Ueno, N., and Satoh, N. (1997). Functional analysis of an ascidian homologue of vertebrate Bmp-2/Bmp-4 suggests its role in the inhibition of neural fate specification. *Development* 124, 5149-59.

Miya, T., Morita, K., Ueno, N., and Satoh, N. (1996). An ascidian homologue of vertebrate BMPs-5-8 is expressed in the midline of the anterior neuroectoderm and in the midline of the ventral epidermis of the embryo. *Mech Dev* 57, 181-90.

.Montgomery, M. K., Xu, S., and Fire, A. (1998). RNA as a target of double-stranded RNA-mediated genetic interference in Caenorhabditis elegans. *Proc Natl Acad Sci U S A* 95, 15502-7.

Morita, K., Chow, K. L., and Ueno, N. (1999). Regulation of body length and male tail ray pattern formation of Caenorhabditis elegans by a member of TGF-β family. *Development* 126, 1337-1347.

Nakao, A., Afrakhte, M., Moren, A., Nakayama, T., Christian, J. L., Heuchel, R., Itoh, S., Kawabata, M., Heldin, N. E., Heldin, C. H., and ten Dijke, P. (1997). Identification of Smad7, a TGFbeta-inducible antagonist of TGF-beta signalling *Nature* 389, 631-5

Nellen, D., Affolter, M., and Basler, K. (1994). Receptor serine/threonine kinases implicated in the control of Drosophila body pattern by decapentaplegic. *Cell* 78, 225-237.

Nellen, D., Burke, R., Struhl, G., and Basler, K. (1996). Direct and long-range action of a DPP morphogen gradient. *Cell* 85, 357-68.

Nikaido, M., Tada, M., Saji, T., and Ueno, N. (1997). Conservation of BMP signaling in zebrafish mesoderm patterning. *Mech Dev* 61, 75-88.

Obara-Ishihara, T., Kuhlman, J., Niswander, L., and Herzlinger, D. (1999). The surface ectoderm is essential for nephric duct formation in intermediate mesoderm. *Development* 126, 1103-1108.

Oh, S. P., and Li, E. (1997). The signaling pathway mediated by the type IIB activin receptor controls axial patterning and lateral asymmetry in the mouse. *Genes Dev* 11, 1812-26.

Padgett, R. W., Das, P., and Krishna, S. (1998). TGF-beta signaling, Smads, and tumor suppressors. *Bioessays* 20, 382-90.

Padgett, R. W., St, J. R., and Gelbart, W. M. (1987). A transcript from a Drosophila pattern gene predicts a protein homologous to the transforming growth factor-beta family. *Nature* 325, 81-4.

Panganiban, G. E., Rashka, K. E., Neitzel, M. D., and Hoffmann, F. M. (1990). Biochemical characterization of the Drosophila dpp protein, a member of the transforming growth factor beta family of growth factors. *Mol Cell Biol* 10, 2669-77.

Patterson, G. I., Koweek, A., Wong, A., Liu, Y., and Ruvkun, G. (1997). The DAF-3 smad protein antagonizes TGF-beta-related receptor signaling in the Caenorhabditis elegans dauer pathway. *Genes Dev* 11, 2679-90.

Piccolo, S., Sasai, Y., Lu, B., and De Robertis, E. M. (1996). Dorsoventral patterning in Xenopus: inhibition of ventral signals by direct binding of chordin to BMP-4. Cell *86*, 589-98.

Raftery, L. A., Twombly, V., Wharton, K., and Gelbart, W. M. (1995). Genetic screens to identify elements of the decapentaplegic signaling pathway in Drosophila. *Genetics* 139, 241-254.

Ren, P., Lim, C. S., Johnsen, R., Albert, P. S., Pilgrim, D., and Riddle, D. L. (1996). Control of C. elegans larval development by neuronal expression of a TGF-beta homolog. *Science* 274, 1389-91.

Ruberte, E., Marty, T., Nellen, D., Affolter, M., and Basler, K. (1995). An absolute requirement for both the type II and type I receptors, punt and thick veins, for Dpp signaling in vivo. *Cell* 80, 889-897.

Salser, S. J., and Kenyon, C. (1996). A C. elegans Hox gene switches on, off, on and off again to regulate proliferation, differentiation and morphogenesis. *Development* 122, 1651-61.

Sampath, T. K., Rashka, K. E., Doctor, J. S., Tucker, R. F., and Hoffmann, F. M. (1993). Drosophila transforming growth factor beta superfamily proteins induce endochondral bone formation in mammals. *Proc Natl Acad Sci U S A* 90, 6004-8.

Savage, C., Das, P., Finelli, A. L., Townsend, S. R., Sun, C. Y., Baird, S. E., and Padgett, R. W. (1996). Caenorhabditis elegans genes sma-2, sma-3, and sma-4 define a conserved family of transforming growth factor beta pathway components. *Proc Natl Acad Sci U S A* 93, 790-4.

Schackwitz, W. S., Inoue, T., and Thomas, J. H. (1996). Chemosensory neurons function in parallel to mediate a pheromone response in C. elegans. *Neuron* 17, 719-28.

Schulte-Merker, S., Smith, J. C., and Dale, L. (1994). Effects of truncated activin and FGF receptors and of follistatin on the inducing activities of BVg1 and activin: does activin play a role in

mesoderm induction? *Embo J* 13, 3533-41.

Sulston, J. E., Albertson, D. G., and Thomson, J. N. (1980). The Caenorhabditis elegans male: postembryonic development of nongonadal structures. *Dev Biol* 78, 542-76.

Sulston, J. E., Schierenberg, E., White, J. G., and Thomson, J. N. (1983). The embryonic cell lineage of the nematode Caenorhabditis elegans. *Dev Biol* 100, 64-119

Suzuki, A., Thies, R. S., Yamaji, N., Song, J. J., Wozney, J. M., Murakami, K., and Ueno, N. (1994). A truncated bone morphogenetic protein receptor affects dorsal-ventral patterning in the early Xenopus embryo. *Proc Natl Acad Sci U S A* 91, 10255-10259.

Suzuki, Y., Yandell, M. D., Roy, P. J., Krishna, S., Savage-Dunn, C., Ross, R. M., Padgett, R. W., and Wood, W. B. (1999). A BMP homolog acts as a dose-dependent regulator of body size and male tail patterning in caenorhabditis elegans. *Development* 126, 241-50.

ten Dijke, P., Yamashita, H., Sampath, T. K., Reddi, A. H., Estevez, M., Riddle, D. L., Ichijo, H., Heldin, C. H., and Miyazono, K. (1994). Identification of type I receptors for osteogenic protein-1 and bone morphogenetic protein-4. J Biol Chem 269, 16985-8.

The C. elegans Sequencing Consortium. (1998). Genome sequence of the nematode C. elegans: a platform for investigating biology. *Science* 282, 2012-2046

Thomas, J. H., Birnby, D. A., and Vowels, J. J. (1993). Evidence for parallel processing of sensory information controlling dauer formation in Caenorhabditis elegans. *Genetics* 134, 1105-17.

Thomsen, G., Woolf, T., Whitman, M., Sokol, S., Vaughan, J., Vale, W., and Melton, D. A. (1990). Activins are expressed early in Xenopus embryogenesis and can induce axial mesoderm and anterior structures. *Cell* 63, 485-93.

Wang, B.B., Muller-Immergluck, M.M., Austin, J., Robinson, N.T., Chisholm, A., and Kenyon, C. (1993). A momeotic gene cluster patterns the anteroposterior body axis of *C. elegans*. Cell 74,29-42

Wang, T., Donahoe, P. K., and Zervos, A. S. (1994). Specific interaction of type I receptors of the TGF-beta family with the immunophilin FKBP-12. *Science* 265, 674-6.

Wang, T., Li, B. Y., Danielson, P. D., Shah, P. C., Rockwell, S., Lechleider, R. J., Martin, J., Manganaro, T., and Donahoe, P. K. (1996). The immunophilin FKBP12 functions as a common inhibitor of the TGF beta family type I receptors. *Cell* 86, 435-44

Weeks, D. L., and Melton, D. A. (1987). A maternal mRNA localized to the vegetal hemisphere in

Xenopus eggs codes for a growth factor related to TGF-beta. *Cell* 51, 861-7.

White, J. G., Southgate, E., Thomson, J. N., and Brenner, S. (1986). The structure of nervous system of the nematode Caenorhabditis elegans. *Philos. Trans. R. Soc. Lond. B Biol. Sci.* 314, 1-340.

Wiersdorff, V., Lecuit, T., Cohen, S. M., and Mlodzik, M. (1996). Mad acts downstream of Dpp receptors, revealing a differential requirement for dpp signaling in initiation and propagation of morphogenesis in the Drosophila eye. *Development* 122, 2153-2162.

Wood, W. B. and the Community of C. elegans Researchers, edu. (1988). The nematode Caenorhabditis elegans. Cold Spring Harbor Press. NY.

Wrana, J. L., Attisano, L., Carcamo, J., Zentella, A., Doody, J., Laiho, M., Wang, X. F., and Massague, J. (1992). TGF beta signals through a heteromeric protein kinase receptor complex. *Cell* 71, 1003-14.

Wrana, J. L., Attisano, L., Wieser, R., Ventura, F., and Massague, J. (1994). Mechanism of activation of the TGF-beta receptor. *Nature* 370, 341-7.

Yamashita, H., ten Dijke, P., Huylebroeck, D., Sampath, T. K., Andries, M., Smith, J. C., Heldin, C. H., and Miyazono, K. (1995). Osteogenic protein-1 binds to activin type II receptors and induces certain activin-like effects. *J Cell Biol* 130, 217-26.

Yandell, M. D., Edgar, L. G., and Wood, W. B. (1994). Trimethylpsoralen induces small deletion mutations in Caenorhabditis elegans. *Proc Natl Acad Sci U S A* 91, 1381-5.

Zhang, Y., and Emmons, S. W. (1995). Specification of sense-organ identity by a Caenorhabditis elegans Pax-6 homologue. *Nature* 377, 55-9.

Zhou, X., Sasaki, H., Lowe, L., Hogan, B. L., and Kuehn, M. R. (1993).
Nodal is a novel TGF-beta-like.gene expressed in the mouse node during gastrulation. *Nature* 361, 543-7.

Zimmerman, L. B., De Jesus-Escobar, J. M., and Harland, R. M. (1996). The Spemann organizer signal noggin binds and inactivates bone morphogenetic protein 4. Cell *86*, 599-606

Zwaal, R. R., Broeks, A., van Meurs, J., Groenen, J. T., and Plasterk, R. H. (1993). Target-selected gene inactivation in Caenorhabditis elegans by using a frozen transposon insertion mutant bank. *Proc Natl Acad Sci U S A* 90, 7431-5.

Acknowledgment

I wish first to thank Drs. Naoto Ueno, Masaharu Noda, Tetsuo Yamamori, Isao Katsura and other members of the laboratory for generous support. I also thank for Drs. Yo Suzuki, William Bill Wood for helpful discussion, also for providing BW185, BC227 strains, Alan Coulson for cosmid clones, Andrew Fire for pPD95.69. Ikue Mori and Yasumi Ohshima for the gift of pJM23 and *lin-15* strains, Ikue Mori also for the identification of the *cet-1::GFP* expressed cells of amphid neuron, Takeshi Ishihara and Isao Katsura for the gift of *GFP-myo-3* vector, Richard W. Padgett for helpful discussion, and for *sma-6* strain, Ruth Yu for critical reading of the manuscript, Henry F. Epstein for helpful discussion. Some nematode strains used in this study were provided by the Caenorhabditis Genetics Center, which is funded by the National Institute of Health, National Center for Research Resources. Many thanks are also extended to all the members of National Institute for Basic Biology and Faculty of Pharmaceutical Sciences, Hokkaido University. This Research was supported by grants from the 'Research for the Future' program of Japan Society for the Promotion of Science to Naoto Ueno.

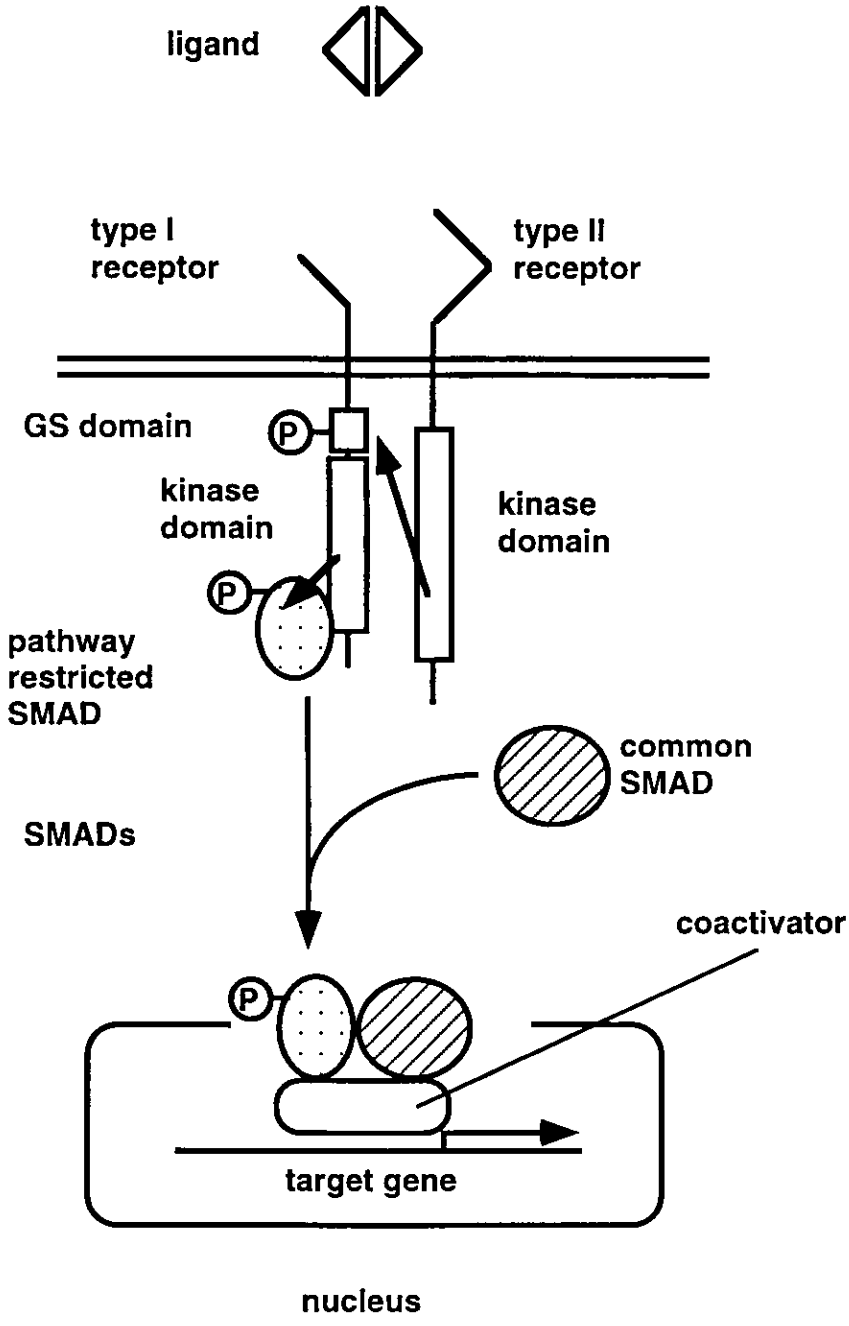

Figure 1-1. TGF-β Superfamily Signaling Pathway.

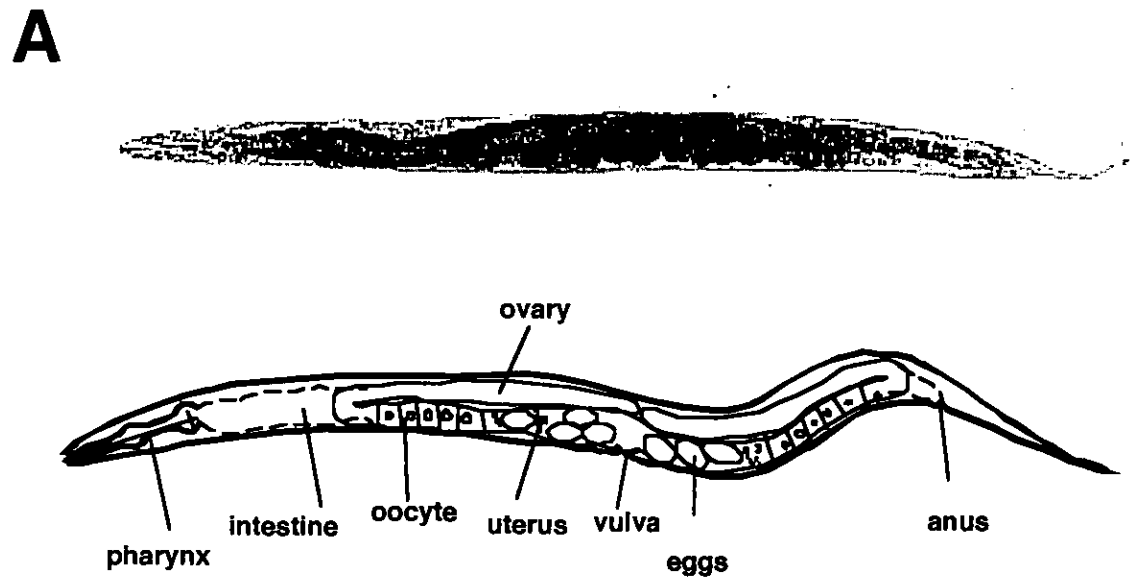

Figure 1-2. The Nematode *Caenorhabditis elegans* as a Model Animal.

(A) Photograph of C. *elegans* adult hermaphrodite (above) and its schematic diagram (below). (B) The life cycle of C. *elegans*. The starvation or overcrowding condition induce animals to the formation of dauer larva instead of L3 larva. (C) Genetic pathway for dauer formation.

A

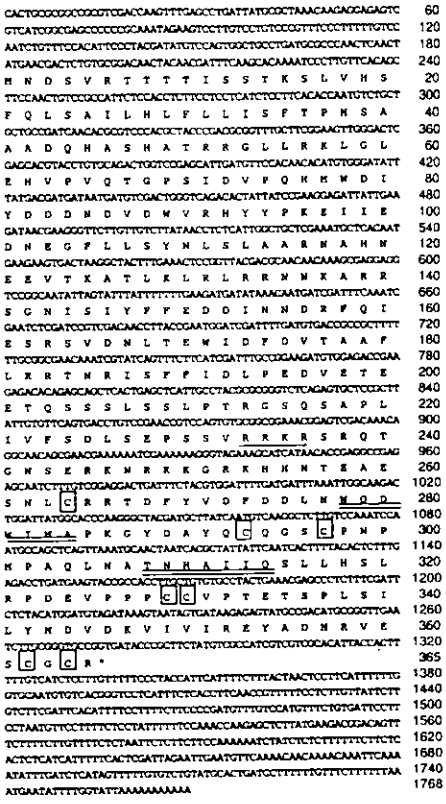

B

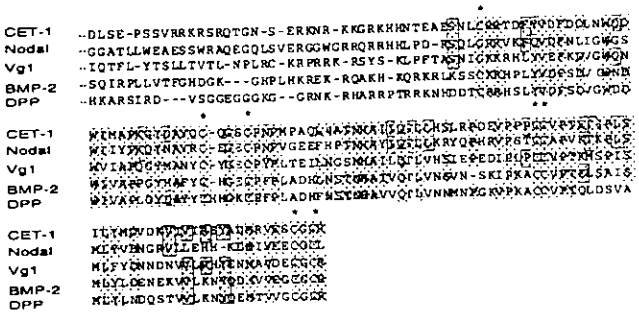
CET-1
Nodal
Vg1
BMP-2
DPP

C

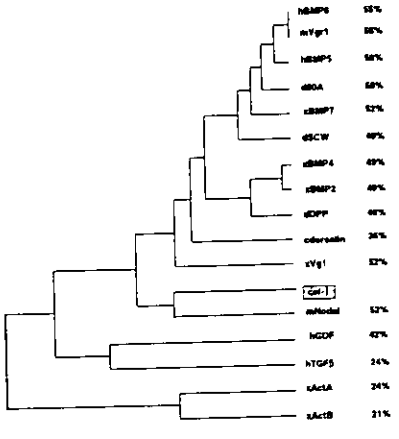
hBMP6
mVg1
hBMP5
dpp
xBMP7
dpCW
xBMP4
xBMP2
xDPP
colorectin
xVg1
Cet-1
mNodal
hGDF
hTGF5
xActA
xActB

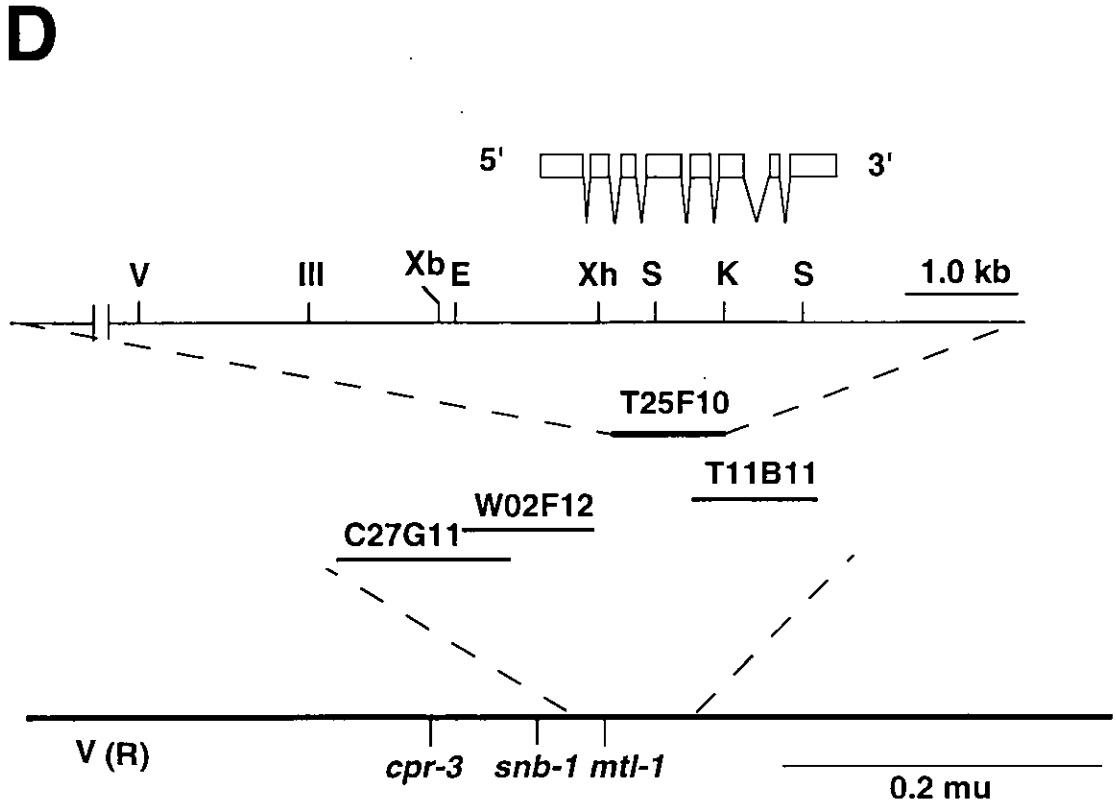

Figure 2-1. Structural Analysis of *cet-1*.

A) Nucleotide and predicted amino acid sequences of *cet-1* cDNA. Nucleotide and amino acid number are indicated at the right. The seven cysteine residues conserved among the TGF-β superfamily members are boxed. The degenerate oligonucleotide primers that were used for cloning of *cet-1* are underlined. The potential N-linked glicosylation site is indicated by double underline. B) Alignment of the C-terminal amino acid sequences of CET-1 and representative members of the TGF-β superfamily. Residues that are conserved in at least 3 of 5 proteins are shaded and the seven conserved cysteine residues are marked with asterisks. Gaps introduced to optimize the alignment are represented by dashes. C) A phylogenetic tree was constructed based on the amino acid sequence similarities of the C-terminal region after the first cysteine residue in the C-termini. D) Physical and genetic maps of the *cet-1* region. The top line is the gene structure with exons represented by boxes, separated by introns. The second line depicts the restriction map of the genomic cosmid clone T25F10. Restriction sites are shown for *Eco* RI (E), *Eco* RV (V), *Hin*d III (III), *Kpn* I (K), *Sac* I (S), *Xba* I (Xb), and *Xho* I (Xh). The third line is the physical map indicating the location of cosmid clones. The fourth line is the genetic map of *cet-1* on linkage group V.

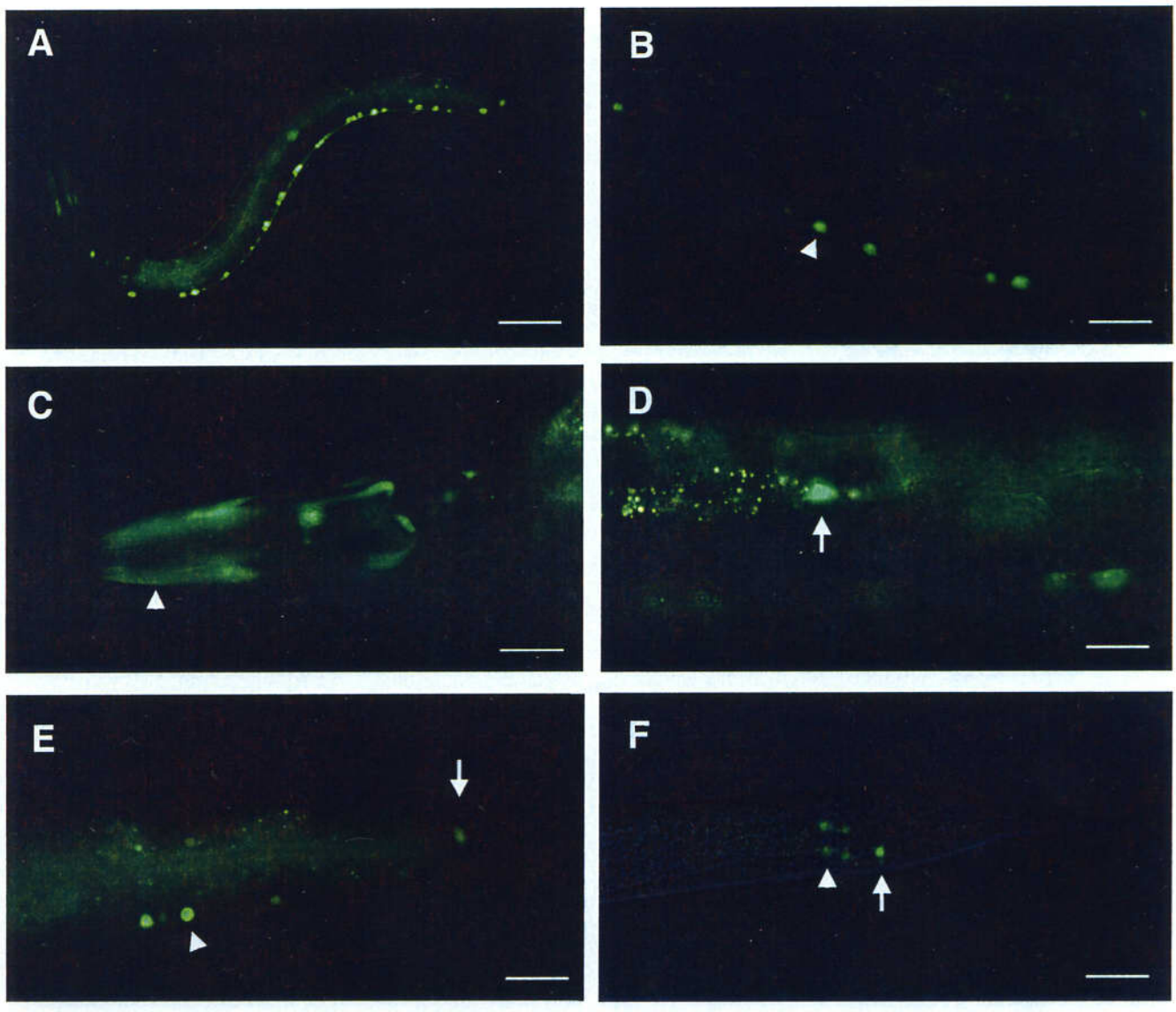

Figure 2-2. Expression Pattern of CET-1 as Studied with a *cet-1::GFP* Fusion Gene.

A) Fluorescence image of L2 larva. Lateral view. Strong signals are seen in the ventral nerve cord (VNC), and canal-associated neurons (CAN). B) *cet-1::GFP* expression in the VNC and C) in the head of adult animals. Body wall muscles (arrowhead), pharyngeal neurons and amphid neuron, AFD show GFP flourescence. D) Cell body of a CAN (arrow). E) Tail region of adult hermaphrodite. VNC (arrowhead) and DVA neuron (arrow) are positive. F) Tail region of L4 male. Two pairs of spicule associated neurons (arrow), and DVA neuron (arrowhead) are detected. All images are taken using fluorescence microscopy. Anterior is to the left and dorsal is up except F), which are ventral view. Scale bars (A) 50 μm, (B-F) 20 μm.

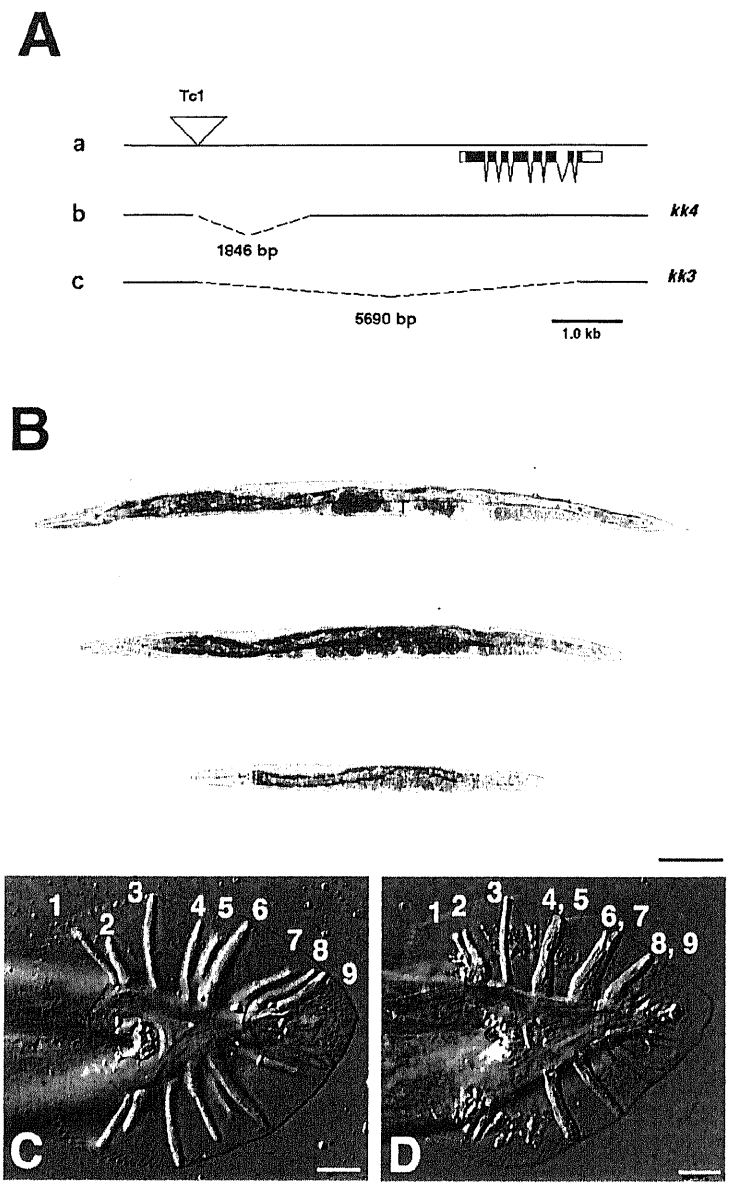

Figure 2-3. *cet-1* Null Mutant.

Inactivation of *cet-1*. To isolate the *cet-1* null mutant, we used targeted gene inactivation by screening for insertion and deletion of Tc1 transposable elements in the *cet-1* region using PCR. A), a) The position of the Tc1 insertion in *cet-1* is indicated above the genomic structure. Tc1 was inserted 4081 bp upstream of the first methionine of *cet-1*. b) *kk4* was identified to be a 1846 bp deletion of *cet-1* 5' upstream region. c) *kk3* was identified to be a 5728 bp deletion that extended from the Tc1 insertion site to encompass the entire *cet-1* cording region. B) Photomicrographs of adult hermaphrodite 5-days old after hatching. N2; *kkEx10[cet-1(+)]* (top), N2 wild type (middle), and *cet-1(kk3)* mutant (below). Lateral view. Anterior is to left and dorsal is up. Scale bars = 100 μm. ; bright-field illumination. C) Male tail phenotype of adult *him-5(e1467)* animal. D) Male tail phenotype of *cet-1(kk3); him-5(e1467)* double mutant. Rays 4 and 5, ray 6 and 7 as well as ray 8 and 9 are fused with each other, respectively. C, D) Photographs of male tails are from Nomarski differential interference contrast microscopy. Scale bars = 10 μm.

Table 2-1. Body Length of Mutants

Mutant	[a]Body length (mm)	[b]N
N2	1.28 ± 0.03	85
kk4	1.27 ± 0.04	67
daf-7(m62)	1.28 ± 0.04	68
cet-1(kk3)	0.75 ± 0.03	103
sma-2(e502)	0.73 ± 0.03	57
sma-3(e491)	0.71 ± 0.03	134
sma-4(e729)	0.79 ± 0.02	86
daf-4(m63)	0.82 ± 0.05	75
daf-7(m62); cet-1(kk3)	0.76 ± 0.04	88
cet-1/+	1.12 ± 0.04	48
[c]*cet-1(kk3); Ex8[cet-1(+) 10:1]*	1.15 ± 0.07	87
[d]*cet-1(kk3); Ex9[cet-1(+) 100:1]*	1.04 ± 0.10	100
N2; *Ex10[cet-1(+)]*	1.43 ± 0.04	58
lon-1(e185)	1.45 ± 0.06	87

Body length were measured of various mutants of 5-day old hatched adult hermaphrodite, with objective microscopy and micrometer.

[a]Data are means ± SD. [b]Numbers of measured animals.

[c]High concentration of plasmids of *cet-1* rescuable fragment were injected.

[d]Low concentration of plasmids of *cet-1* rescuable fragment were injected

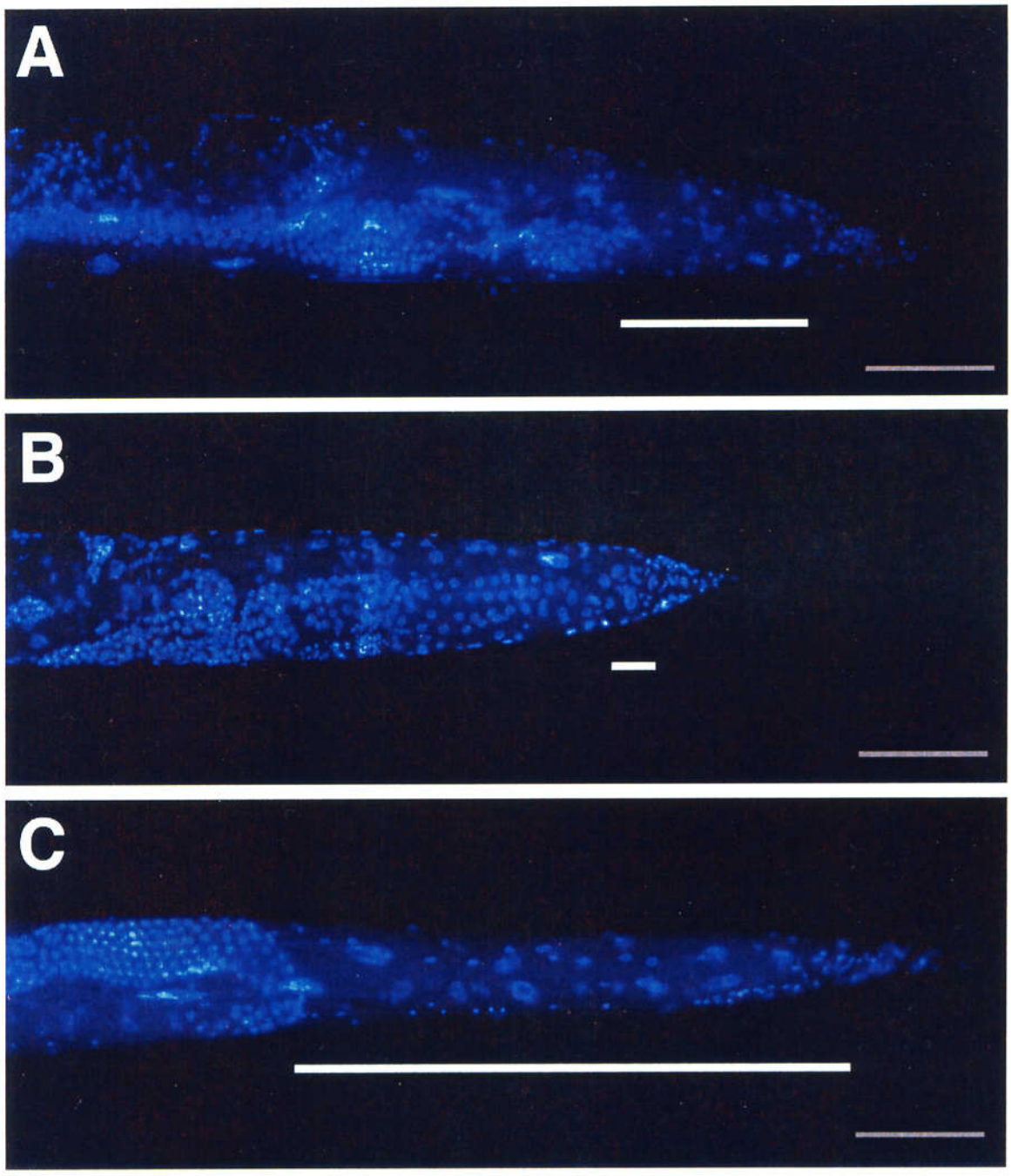

Figure 2-4. Regional Difference of the Worms with Change in CET-1 Dosage.

Photographs from fluorescent microscopy of tail region of 5-day old adult hermaphrodite stained with DAPI. (A) N2. (B)*cet-1(kk3)*. (C) N2; *EX10[cet-1(+)]*. The regions from the gonad arms to anus are indicated by bars. Lateral views. Anterior is at left and dorsal is up. Scale bars = 10 μm.

Table 2-2 Length of Body Parts

Genotype	Length (mm)				
	Pharynx	Pharynx to Gonad	Gonad	Gonad to Anus	[c]Total
N2 wild type	[a]0.14 ± 0.01 [b](11)	0.10 ± 0.03 (8)	0.77 ± 0.04 (60)	0.10 ± 0.01 (8)	1.28 (100)
cet-1(kk3)	0.12 ± 0.01 (9)	0.02 ± 0.01 (2)	0.45 ± 0.04 (35)	0.04 ± 0.01 (3)	0.75 (57)
N2; *Ex10[cet-1(+)]*	0.16 ± 0.01 (13)	0.28 ± 0.04 (22)	0.64 ± 0.09 (50)	0.24 ± 0.05 (19)	1.43 (112)

Length of body parts were measured of N2, *cet-1(kk3)*, N2; *Ex10[cet-1(+)]* mutants of hatched after 5-days old adult hermaphrodite with objective microscopy and micrometer.

[a]Data are means ± SD.

[b]Relative percentage to the N2 total length.

[c]Total not contain the length of tail.

Table 2-3 Frequency of Male Tail Ray Fusions in Mutants (%)

Mutant	Ray 1	Ray 2	Ray 3	Ray 4	Ray 5	Ray 6	Ray 7	Ray 8	Ray 9	[a]N
cet-1(kk3)	0	0	0	46	47	85	85	18	18	153
sma-2(e502)	0	0	0	22	22	70	70	12	12	86
sma-3(e491)	0	0	0	18	19	54	53	11	11	74
sma-4(e729)	0	0	0	30	30	68	68	9	9	53
daf-4(m63)	0	0	0	24	30	63	63	15	13	46

The frequency in percent at which each ray is fused with another ray.

[a]Numbers of sides scored.

Table 2-4 Epistatsis Analysis of *mab-21* with *sma-2, sma-3, sma-4, sma-6, daf-4* and *cet-1*

Genotype	Male tail phenotype	
	Thin ray 6, ray 4, 6 fusion (Mab-21)	Thick ray 4,5,6,7 (Cet-1/Sma/Daf-4)
mab-21(bx53); him-5(e1490)	+ [a](>500)	-
mab-21(bx53); sma-2(e502); him-5(e1490)	+ (350)	-
mab-21(bx53); sma-3(e491); him-5(e1490)	+ (300)	-
mab-21(bx53); sma-4(e491); him-5(e1490)	+ (300)	-
mab-21(bx53); daf-4(e491); him-5(e1490)	+ (250)	-
sma-6(wk7); mab-21(bx53); him-5(e1490)	+ (150)	-
mab-21(sy155); cet-1(kk3); him-5(e1467)	+ (50)	-

[a]Numbers of animals scored given in parentheses.

Table 2-5. Dauer Formation of *daf-7; cet-1(kk3)* Double Mutants

Genotype	Percent of dauer formation	
	20 ℃	25 ℃
daf-7(e1372)	[a]21 (777)	100 (796)
daf-7(m62)	21 (624)	100 (720)
daf-7(e1372); cet-1(kk3)	77 (673)	100 (606)
daf-7(m62); cet-1(kk3)	56 (595)	100 (279)
daf-4(m63)	63 (364)	100 (432)
cet-1(kk3)	0 (480)	0 (226)
daf-7(e1372); sma-2(e502)	40 (206)	100 (160)
daf-7(m62); sma-2(e502)	29 (231)	100 (202)

[a]The percentage of animals forming dauers is given, with the total number of animals counted given in parentheses.

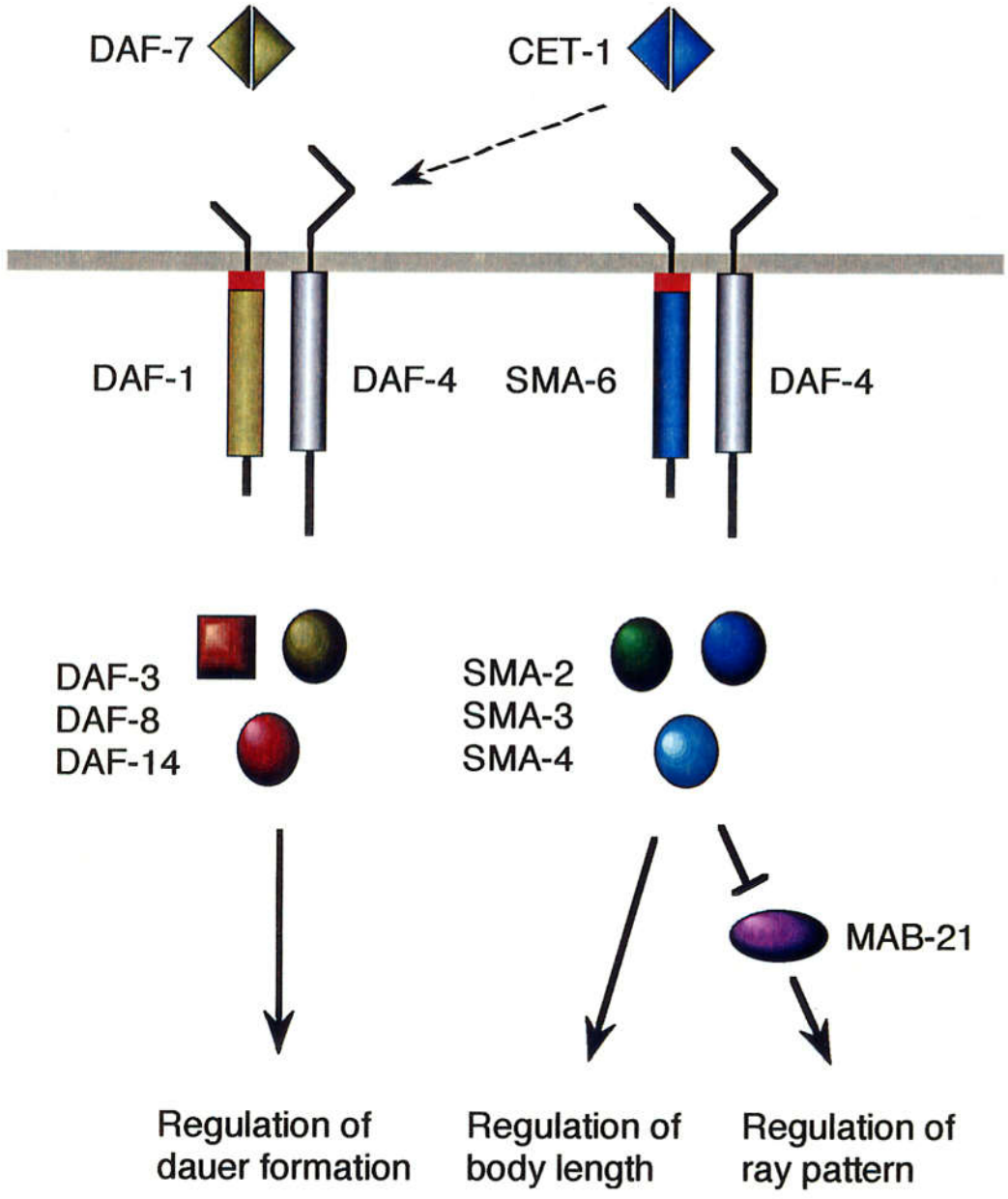

Figure 2-5. Two Distinct TGF-β Signal Pathways in the Nematode *C. elegans*..

Two distinct signaling cascades, the *daf* pathway (regulation of dauer formation) and the *cet-1/sma* pathway (regulation of body length and male tail ray pattern formation) have been identified. A weak functional redundancy was observed between the *daf* and *cet-1/sma* pathways (thin arrow). *mab-21* appears to be negatively regulated by the *cet-1/sma* pathway in the pattern formation of male tail rays.

A

```
tttaattacccaagtttgagaaatgtcggaagaagctgaagctggaccatcgccaaaagt   60
                        M  S  E  E  A  E  A  G  P  S  P  K  V    13
taatggggaaaatggaaacggaacaaatacgttcgacgacttgtacgtggatgacaaaat  120
 N  G  E  N  G  N  G  T  N  T  F  D  D  L  Y  V  D  D  K  M    33
gcgtcgaatgattgtcgaccttcagcgtcaatggctcacggattatcacgatagccgcga  180
 R  R  M  I  V  D  L  Q  R  Q  W  L  T  D  Y  H  D  S  R  E   53
gaaatctctcgttgctctaactgaaaaactccatcaagaattcatggaagatcaggagcg  240
 K  S  L  V  A  L  T  E  K  L  H  Q  E  F  M  E  D  Q  E  R   73
agtccgtcgcgatttgttggttcagttcaagatagagctcgaccagacaaaggaagagct  300
 V  R  R  D  L  L  V  Q  F  K  I  E  L  D  Q  T  K  E  E  L   93
ggagaagaagcacgcggagaatctcaaggaggagattgaaaagctgtcggaaaaacacca  360
 E  K  K  H  A  E  N  L  K  E  E  I  E  K  L  S  E  K  H  Q  113
aagggaacttgctgtcgctaagaagaagcagtggtgctggcaatgcaacagcgaggcaat  420
 R  E  L  A  V  A  K  K  K  Q  W  C  W  Q  C  N  S  E  A  I  133
ctatcattgctgctggaacactgcttattgcagcgttgaatgccaacaaggacactggca  480
 Y  H  C  C  W  N  T  A  Y  C  S  V  E  C  Q  Q  G  H  W  Q  153
gattcatcgcaagttctgccgcagaaagaagagcaacggtggagccccaggaccagttca  540
 I  H  R  K  F  C  R  R  K  K  S  N  G  G  A  P  G  P  V  Q  173
gccaattgctgagcctactcaaagtcaacaatgattgaaacttaaataatatgctatctg  600
 P  I  A  E  P  T  Q  S  Q  Q  *                              183
cgagccggaggccctttgaaaagtaacaaagcttgtgtcaggttttcgaagtttatctca  660
tcacacatcccgttttctgtgttactactgtatatcttctctccaataacatgcaatatt  720
tttctataatcccatgacaacaacaatttttaagatcttctatataaatcctgttaattag  780
gaatttggatcaatttcggagagatctcaaacttgtgttaattccttcgagaaataatca  840
agaaattatgtgaataaagtttatttttgataaaaaaaaaaaaaaaaaaa            888
```

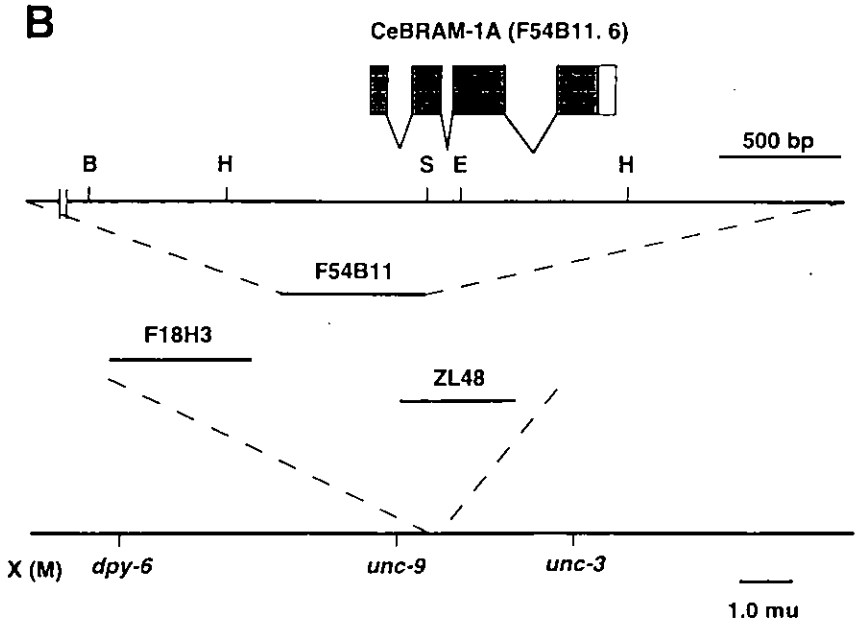

Figure 3-1. Structural Analysis of CeBRAM-1A.

(A) Nucleotide and predicted amino acid sequences of CeBRAM-1A cDNA. Nucleotides are numbered at the end of the lines. Nucleotides in bold characters at the 5′ end are derived from the SL1 trans-spliced leader sequence. The stop codon is marked by an asterisk. (B) Physical and genetic map in the CeBRAM-1A region. The top line is the gene structure with exons as boxes separated by introns. The direction of transcription is from right to left. The second line is the partial restriction map of the genomic cosmide clone F54B11. (B) *Bam* HI; (H) *Hind* III; (S) *Sac* I; (E) *Eco* RI. The third line is the physical map showing the position of cosmid clone F54B11. The fourth line is the genetic map of the portion of the Middle of the X chromosome.

A

```
ttcggcacgaggttaaacccgtgcaaaagatggccgatgggcaagtgcatgatgaattga    60
                              M  A  D  G  Q  V  H  D  E  L  M     11
tgatggatcagcaacaacagcaaggagtggttcctcaacaaggtgatattcacctatcgc   120
  M  D  Q  Q  Q  Q  Q  G  V  V  P  Q  Q  G  D  I  H  L  S  P     31
cgatcgacaaggatctcggagatgcggcgttagaaaataatgtgcggcagtatcatctcg   180
  I  D  K  D  L  G  D  A  A  L  E  N  N  V  R  Q  Y  H  L  D     51
atggagtggtcgtcagtgaagggatgaaacgaatgataatcgacctgcaacgtcattggc   240
  G  V  V  V  S  E  G  M  K  R  M  I  I  D  L  Q  R  H  W  L     71
tcagtgagtatcacgcgtcacgtgagaagtgtcttgtagagcttaccgagaagttgcatc   300
  S  E  Y  H  A  S  R  E  K  C  L  V  E  L  T  E  K  L  H  Q     91
aagaattcatgatggatcaacagaaaattcgatcggaactcttacaacagttcaaagacg   360
  E  F  M  M  D  Q  Q  K  I  R  S  E  L  L  Q  Q  F  K  D  E    111
agttggaacagacaagagccgatctagaaaacaaacacagagagaacttgaagatggaaa   420
  L  E  Q  T  R  A  D  L  E  N  K  H  R  E  N  L  K  M  E  S    131
gtgcaaagttgaatgaaaagcataaaagagagttggttgcatcaagaaagaaacaatggt   480
  A  K  L  N  E  K  H  K  R  E  L  V  A  S  R  K  K  Q  W  C    151
gctggtcgtgtgataatgaggctatataccattgctgctggaataccgcatattgcagtg   540
  W  S  C  D  N  E  A  I  Y  H  C  C  W  N  T  A  Y  C  S  V    171
ttgaatgccaacagggacattggcagactcatcgaaagttttgccgcagaaagaaaggaa   600
  E  C  Q  Q  G  H  W  Q  T  H  R  K  F  C  R  R  K  K  G  N    191
acaatgctcctggagcaccaagtgtaccagctcctcaacaagtcggagcaccaatgccgc   660
  N  A  P  G  A  P  S  V  P  A  P  Q  Q  V  G  A  P  M  P  P    211
cacaacaacaataatttttctttcgttttaactctctaatcatcattatcatcaatctcac   720
  Q  Q  Q  *                                                    214
gtcagaacacgaaactgaataaatttcaaccacccaccaccgcacaaatgcgacgctgat   780
ctcacccaccacgtctatttatattccaaatcctaatgagtttctgttattcttcatctt   840
tatcaatttgtcgaacttttctatgttttccttgttcaataaaaaatttaataaaaaaaaa   900
aaaaaaaaa                                                      909
```

B

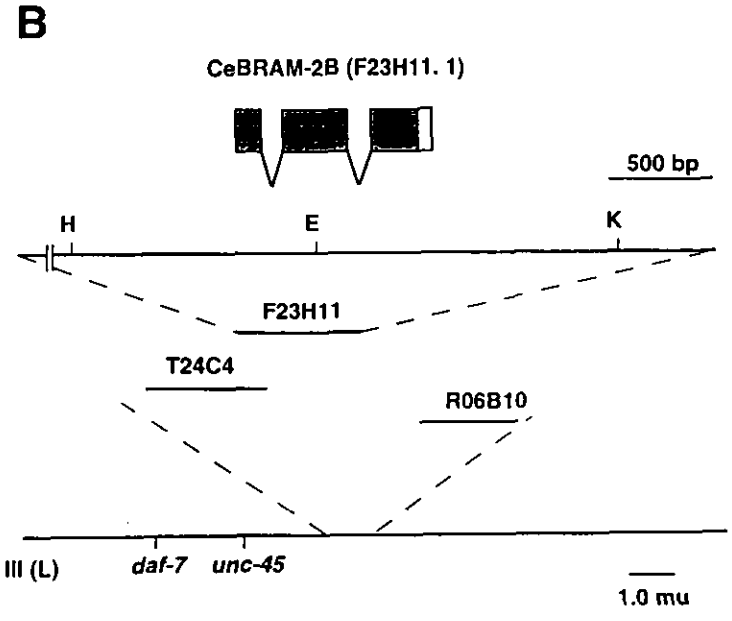

Figure 3-2. Structural Analysis of CeBRAM-2B.

(A) Nucleotide and predicted amino acid sequences of CeBRAM-2B cDNA. Nucleotides are numbered at the end of the lines. The stop codon is marked by an asterisk. (B) Physical and genetic map in the CeBRAM-2B region. The top line is the gene structure with exons as boxes separated by introns. The direction of transcription is from right to left. The second line is the partial restriction map of the genomic cosmid clone F23H11. (H) *Hind* III; (E) *Eco* RI. (K) *Kpn* I. The third line is the physical map showing the position of cosmid clone F23H11. The fourth line is the genetic map of the portion of the left of the chromosome III.

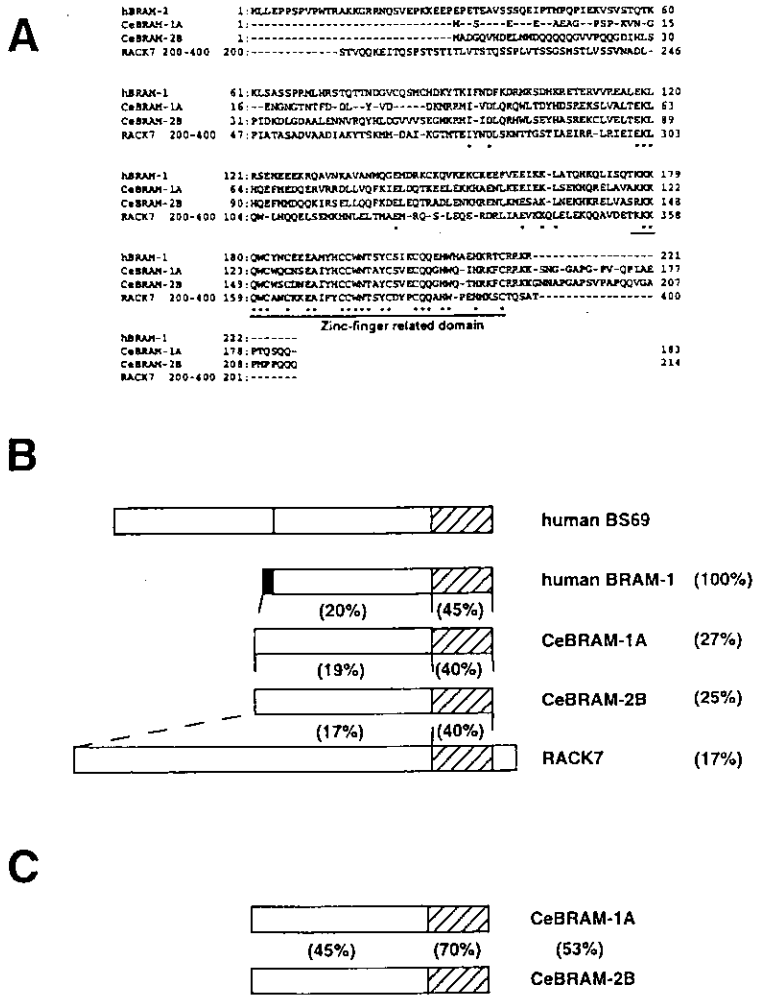

Figure 3-3. Alignment of the Amino Acid Sequence of CeBRAM-1A, CeBRAM-2B, Human BRAM-1 and RACK7.

(A) The amino acid sequence of predicted cording region of *C. elagans* CeBRAM-1A and CeBRAM-2B were aligned with human BRAM-1 (Kurozumi et al., 1998) and amino acid regidue 200-400 of human RACK7 (unpublished and found in GenBank). Gaps introduced to optimize the alignment are represented by dashes. Residues shared by all proteins are marked with asterisks (*). (B) Schematic diagram of the structure of BS69 (human), human BRAM-1, CeBRAM-1A, CeBRAM-2B, and human RACK7. Comparison of predicted human BRAM-1 amino acid identity with CeBRAM-1A, CeBRAM-2B and human RACK7 are indicateed in the reft. Comparison of N-terminal, and C-terminal region of human BRAM-1 amino acid identity with CeBRAM-1A, CeBRAM-2B and human RACK7 are indicateed. (C) Comparison of predicted CeBRAM-1A amino acid identity with CeBRAM-1B are indicated.

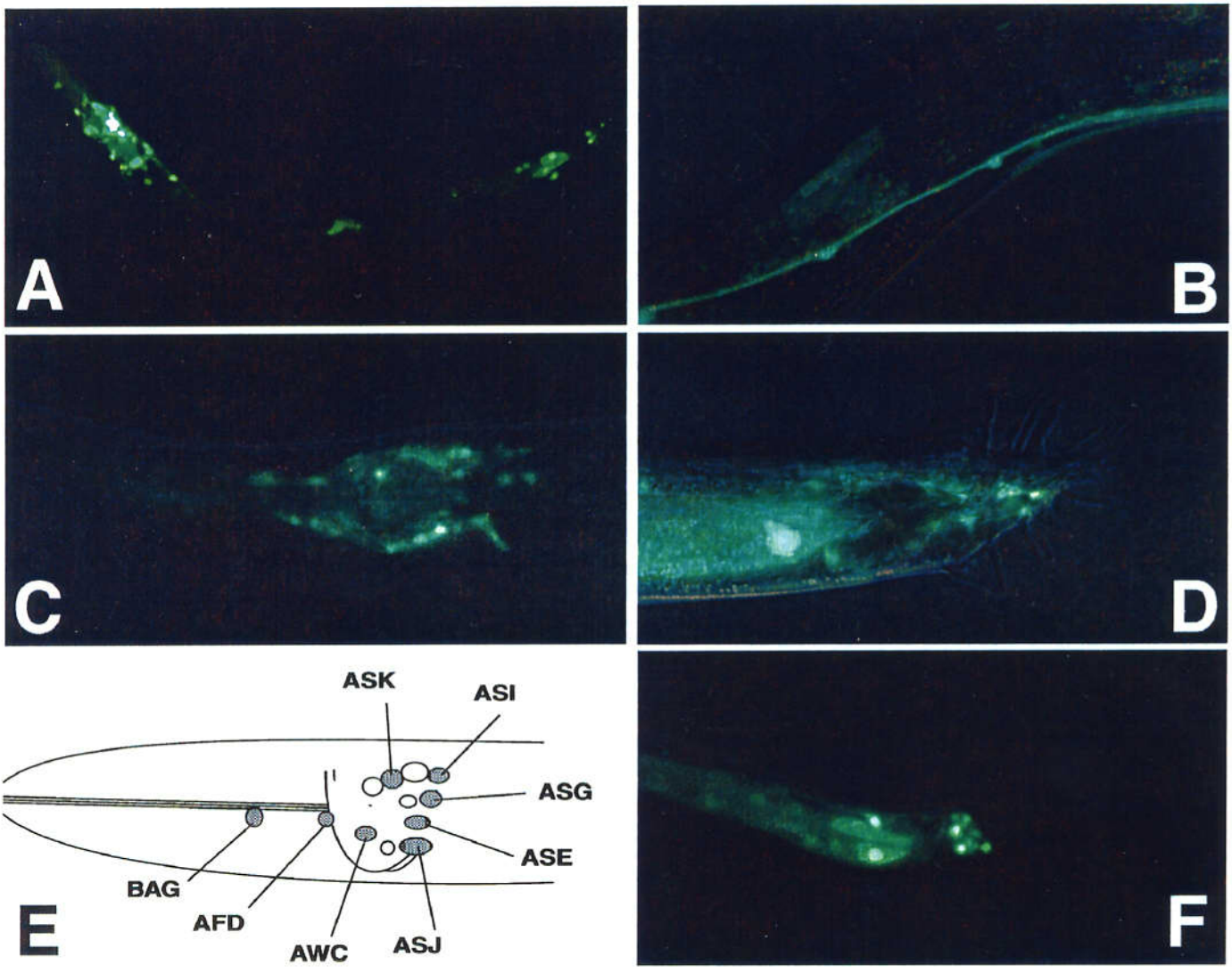

Figure 3-4. Expression of a *CeBRAM-1A::GFP* Fusion.

(A) *CeBRAM-1A::GFP* expression of L3 hermaphrodite. Strong expression were seen in head region and tail region of animal. (B) Strong signals are seen in the ventral nerve cord (VNC). (C) Lateral view of adult hermaphrodite showing GFP expression in the head. GFP fluorescence is seen in the cell bodies of BAG AFD ASK ASI ASG ASE ASJ and AWC neurons. (D) Tail region of adult male. GFP fluorescence is seen in unidentified male specific neurons. (E) A diagram summarizing the GFP-expressing neuron. (F) Tail region of adult hermaphrodite. GFP fluorescence is seen in the cell bodies of PHA and PHB phasmid neurons. Anterior is to the left, and dorsal is up.

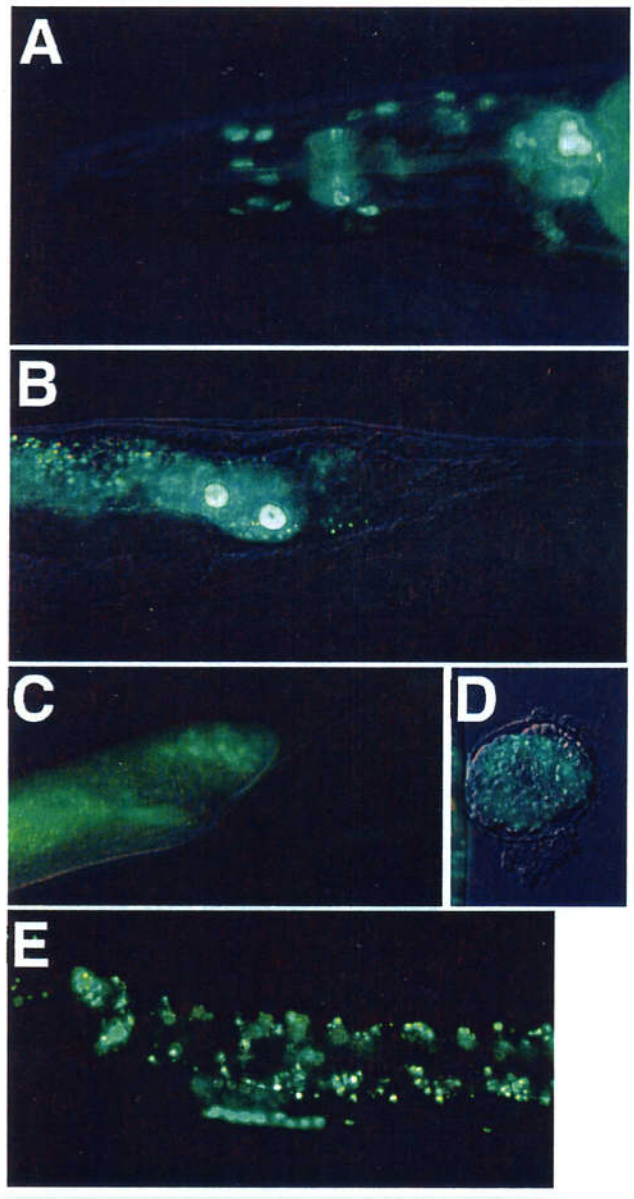

Figure 3-5. Expression of a *CeBRAM-2B::GFP* Fusion.

(A) *CeBRAM-2B::GFP* expression of the head region of adult hermaphrodite. GFP fluorescence is seen in the cell bodies of pharyngeal muscle. (B) Tail region of L4 hermaphrodite. GFP fluorescence is seen in the gut cells. (C) Tail region of L4 mail. Male specific expression was seen in the unidentified precursor cells of the rays. (D) Comma stage embryo. GFP expression was detected at the early stage of embryo. (E) Vulval region of adult hermaphrodite. Fluorescence is seen in the ventral nerve cord (VNC).

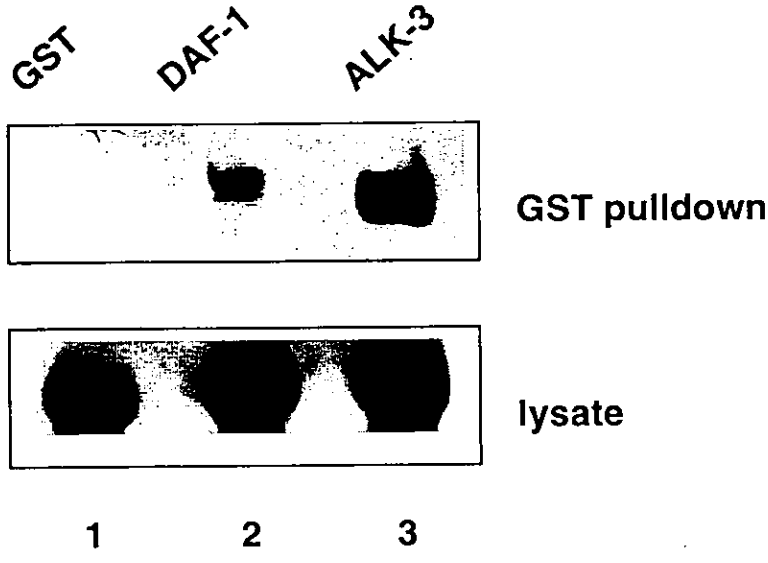

Figure 3-6. CeBRAM-1A Associates with DAF-1 Type I Receptor.

COS7 cells were transiently transfected with cDNAs of hemagglutinin (HA)-CeBRAM-1 and with GST-DAF-1 or GST-BMPR-IA. GST-DAF-1 as well as GST-BMPR-IA fusion proteins were efficiently immunoprecipitated with anti-HA anti body, through the binding to HA-tagged CeBRAM-1.

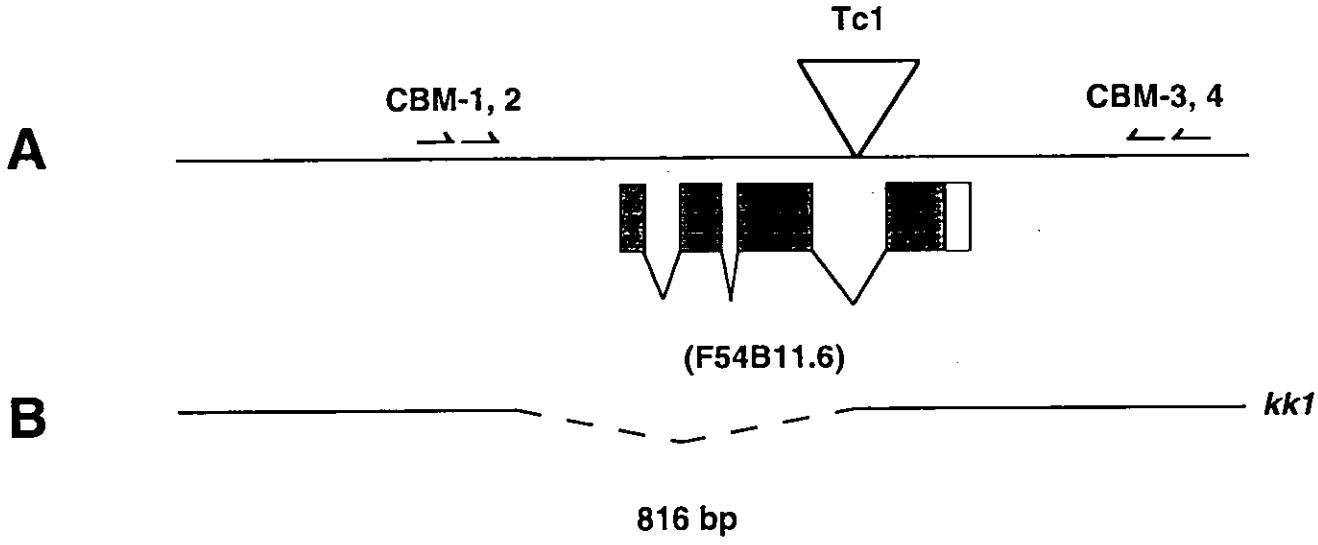

Figyre 3-7. Isolation and Characterization of CeBRAM-1A Null Mutant.

To isolate the CeBRAM-1A null mutant, I used targeted gene inactivation by screening for insertion and deletion of Tc1 transposable elements in the CeBRAM-1A region using PCR. (A) The position of the Tc1 insertion in CeBRAM-1A is indicated above the genomic structure. (B) CeBRAM-1A mutant *(kk1)*. The genomic structure of *kk1*, that deleted 816 bp of the entire region that covers exon 1 to exon 3 of CeBRAM-1A cording region.

Table 3-1. Genetic Interaction of CeBRAM-1A with *daf-7* TGF-β Pathway Mutants

	15 ℃		20 ℃		23 ℃		25 ℃	
	+	BRAM	+	BRAM	+	BRAM	+	BRAM
daf-1 m40	0 (132)	0 (242)	14 (137)	2 (373)	66 (185)	10 (348)	100 (317)	51 (495)
m402	2 (291)	0 (179)	61 (144)	6 (231)	94 (220)	24 (329)	100 (481)	72 (750)
m213	0 (244)	0 (126)	92 (381)	27 (245)	95 (440)	37 (308)	100 (614)	80 (482)
daf-7 e1372	2 (177)	0 (170)	60 (210)	4 (316)	98 (295)	52 (261)	100 (493)	89 (335)
m63	N. D.	N. D.	68 (211)	18 (298)	N. D.	N. D.	100 (295)	72 (420)
daf-11 m47	N. D.	N. D.	8 (154)	5 (281)	N. D.	N. D.	56 (1488)	16 (2323)
daf-14 m77	N. D.	N. D.	7 (247)	3 (492)	N. D.	N. D.	47 (1283)	38 (1260)

Percent dauer formation of CeBRAM-1A and the *daf-c* double mutants at various temperatures. The percentage of animals forming dauers is given, with the total number of animals counted given in parentheses. + indicate the *daf-c* single mutants, and BRAM indicates *daf-c;* CeBRAM-1A double mutants.

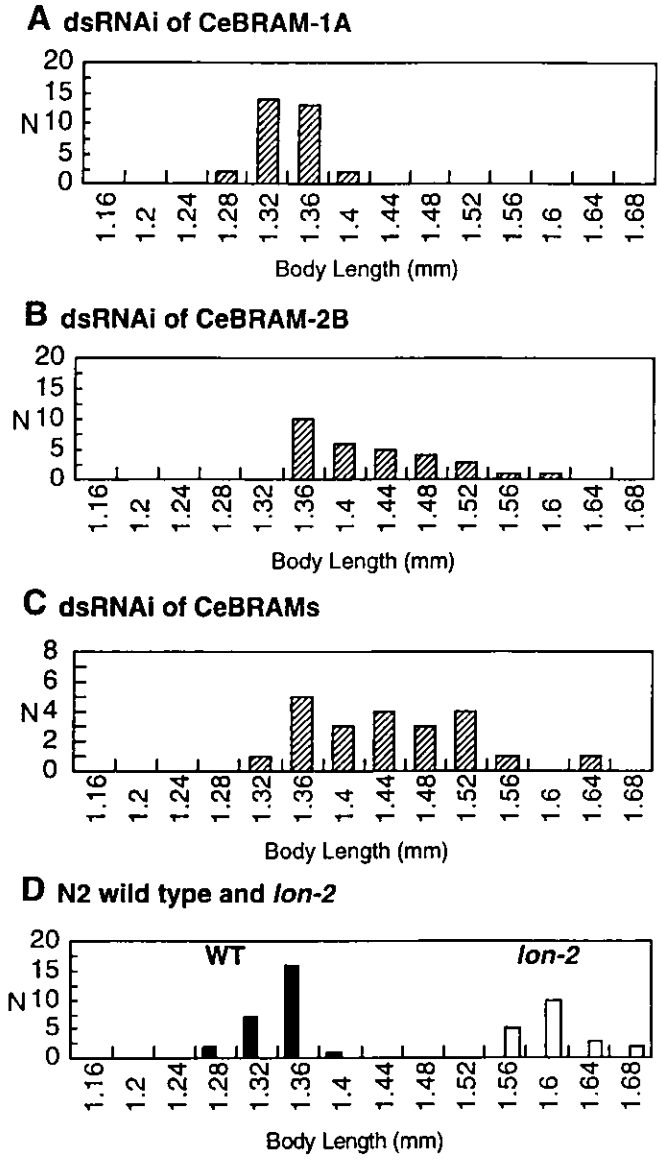

Figure 3-8. dsRNAi of CeBRAM-2B Caused Lon Phenotype.

The effect of dsRNAi of CeBRAM-1A (A), CeBRAM-2B (B), and mixture of CeBRAM-1A and CeBRAM-2B (C), against N2 wild type. F1 progeny of injected animals were grown for 5-days and measured body length. (D) shows the body length of the animals of uninjected N2 wild type and *lon-2* mutant.

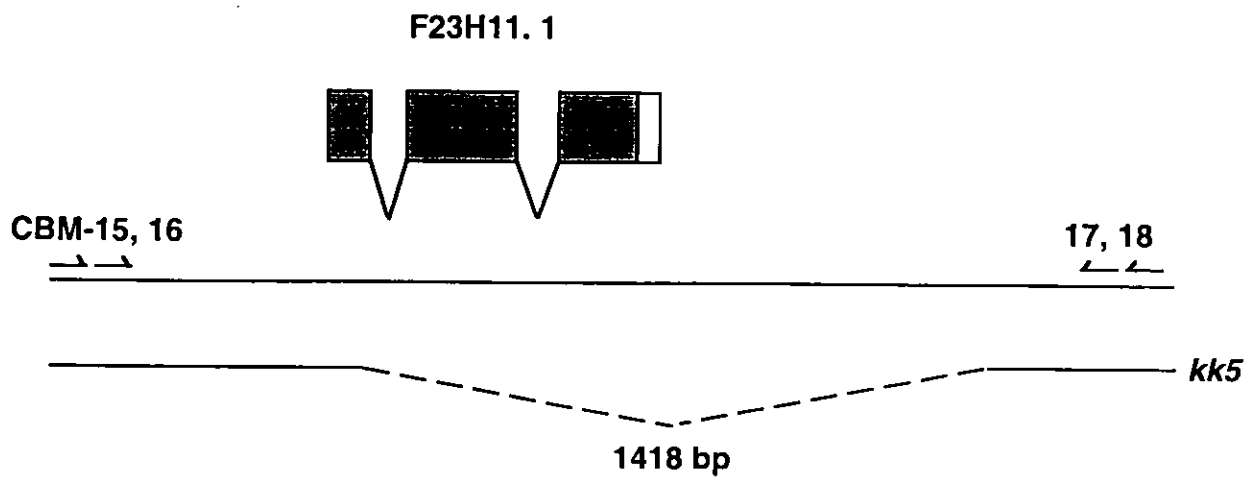

Figure 3-9. Isolation of CeBRAM-2B Null Mutant.

To isolate the CeBRAM-2B null mutant, I used targeted gene inactivation by screening for deletion of chemical mutagenesis by TMP-UV method in the CeBRAM-2B region using PCR. I can isolate the 1418 bp deleted mutant *(kk5)*. Genomic structure of CeBRAM-2B region and CeBRAM-2B mutant *(kk5)*.

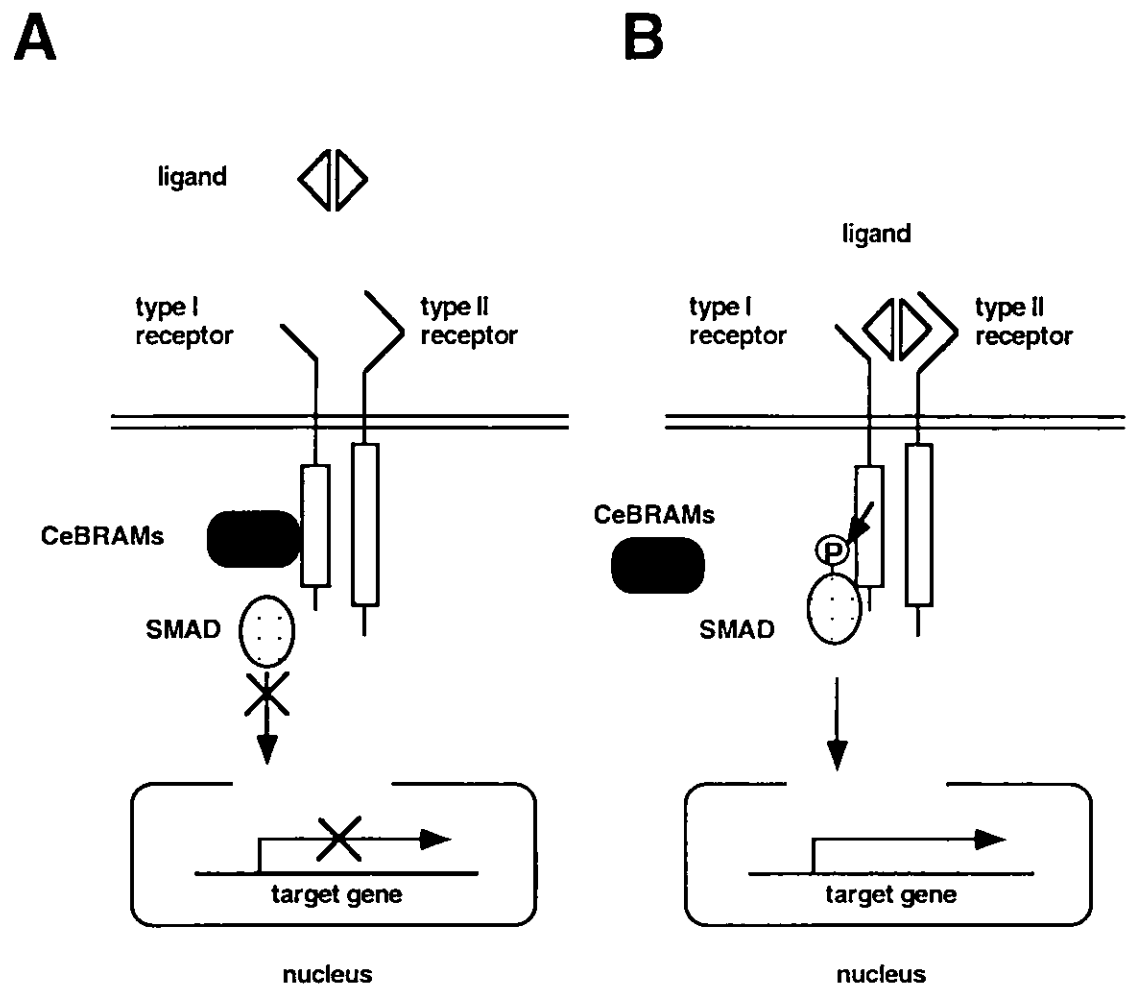

Figure 3-10. Possible Mechanism of Negative Regulation of CeBRAM-1A and CeBRAM-2B in the TGF-β Signaling Pathways in the Nematode *C. elegans*.

(A) When the CeBRAMs associates with type I receptor, SMAD protein can not associate with receptor. (B) When the CeBRAMs dissociates with the receptor, SMAD protein are phosphorylated by type I receptor and translocate to the nucleus.